THESIS

NUMERICAL EVALUATION OF ONE-DIMENSIONAL LARGE-STRAIN CONSOLIDATION OF MINE TAILINGS

Submitted by

Luis Angel Agapito Tito

Department of Civil & Environmental Engineering

In partial fulfillment of the requirements

For the Degree of Master of Science

Colorado State University

Fort Collins, Colorado

Fall 2015

Master's Committee:

Advisor: Christopher A. Bareither
Co-Advisor: Charles D. Shackelford

Sally J. Sutton

ABSTRACT

NUMERICAL EVALUATION OF ONE-DIMENSIONAL LARGE-STRAIN CONSOLIDATION OF MINE TAILINGS

The objective of this study was to evaluate the applicability of commercially-available, one-dimensional (1-D) large-strain consolidation programs (FSConsol and CONDES0) for predicting mine tailings consolidation to estimate storage capacity of tailings storage facilities (TSFs). This study consisted of the following tasks: (i) consolidation modeling of well-known benchmark examples from literature, (ii) parametric study to assess the influence of input parameters (i.e., constitutive relationships, initial void ratio, impoundment geometry, and tailings production rate) on consolidation behavior and storage capacity, and (iii) consolidation and storage capacity prediction for a full-scale copper TSF.

A benchmark example that represented instantaneous deposition of tailings (Townsend and McVay 1990) was evaluated with CONDES0 and FSConsol and indicated that both models are appropriate for predicting the consolidation behavior of tailings that are deposited instantaneously. Both models yielded similar temporal settlement curves and void ratio profiles. A gradual tailings deposition benchmark example (Gjerapic et al. 2008) was evaluated with both programs and suggested that FSConsol was more applicable for problems dealing with continuous discharge of tailings. In particular, FSConsol was more applicable when the tailings discharge rate varied temporally, which is a key constraint to modeling a full-scale TSF.

The parametric study results suggested that the initial tailings void ratio and constitutive relationships (i.e., void ratio versus effective stress, e-σ', and hydraulic conductivity versus void ratio, k-e) had more pronounced effects on consolidation behavior relative to impoundment geometry and tailings production rate. In particular, a comparison between rapidly consolidating

mine tailings (copper tailings) and slowly consolidating mine tailings (mature fine tailings from oil sands) indicated that a decrease in hydraulic conductivity by four orders of magnitude can extend the time required for consolidation by more than 200 yr. Changes in impoundment geometry and tailings production rate had limited effects on impoundment capacity for the range of side slopes (1.0H:1V to 4.5H:1V) and production rates (50 mtpd to 300 mtpd) evaluated in this study.

FSConsol modeling results from the full-scale copper mine TSF were compared to field data and suggest that a 1-D consolidation model can yield a satisfactory prediction of in-situ consolidation behavior of copper tailings. Comparison between the actual average tailings dry density (ρ_d) during the first 4 yr of operation and predicted average ρ_d yielded coefficients of determination (R^2) as high as 81 % and 93 % for Operation and Design assessments, respectively. In addition, predicted tailings height within the TSF showed good agreement with actual impoundment heights for the first 6 yr of operation; R^2 = 99.1 % for the Operation assessment and cyclone operation time (COT) of 70 %, which was the average actual COT. A procedure was developed to predict average ρ_d of a full-scale TSF using a 1-D consolidation model that includes the following considerations: (i) estimate total tailings volume in the TSF based on predicted impoundment height and (ii) use this total volume with dry tailings mass discharged into the TSF to compute ρ_d. The main finding from this study was that the modeling of gradual tailings deposition with FSConsol provides a reliable prediction of impoundment height and impoundment capacity.

ACKNOWLEDGEMENTS

I would like to thank deeply my love Roxana for her dedicated love, support, and care during our time at Colorado State University. Also, I would like to write a note for my courageous daughter Camila. Camila came to Fort Collins when she was around one and a half years old and all the time she showed me to be valiant due to many changes at her early years. I hope when you read this, you could feel all the good memories that we, as a family, spent at Fort Collins.

First, I would like to dedicate this thesis to my parents Luis Alberto Agapito Francia and Concepcion Tito Ccarhuas who are my sources of inspiration and motivation.

Second, I would like to thank my advisor, Dr. Christopher Bareither, who gave me the opportunity to continue my graduate studies, and also provided constant support and guidance throughout my Master's thesis. I would also like to extend my thanks to Dr. Charles Shackelford, who believed in my abilities, and Dr. Sally Sutton for serving on my graduate committee.

Last, but not least, I wish to thank my siblings José Luis, Luis Alberto, and Cecilia for being an inspiration. In particular, I would like to thank Luis Alberto for being a model of perseverance. He is the first and unique member of the family who holds a PhD degree. I hope in the future Camila and José Antonio, my nephew, could pursue a PhD degree.

TABLE OF CONTENTS

Page

LIST OF TABLES

LIST OF FIGURES

CHAPTER 1: INTRODUCTION

Mine tailings are a by-product of metallurgical ore processing that predominantly consist of fine-grained particles with high water content and residual chemicals from ore extraction (e.g., Bussière 2007; Blight 2010). Tailings generally are transported and disposed as slurry into large impoundments called tailings storage facilities (TSFs). The mass and corresponding volume of tailings generated at a given mine currently is increasing due to the increasing prevalence of mining low-grade ores (West 2011). Processing low-grade ores increases the volume of tailings that require management in TSFs. For example, Chuquicamata Mine located in Atacama, Chile produced approximately 161,000 metric tons per day (1 mtpd = 1 Mg/d) of ore production, which generated a comparable mass of tailings following ore extraction (Wels and Robertson 2003).

Understanding and predicting physical and chemical processes of tailings following deposition in TSFs present challenges to the mining community. In particular, consolidation of tailings presents a challenge at nearly all mines due to increasing tailings generation and disposal of tailings as slurry. Consolidation relates to the decrease in volume of tailings that is attributed to discharge of pore water. Thus, high water content, low permeability fine-grained mine tailings can yield large volume reductions and long elapsed times for completion of consolidation (Carrier et al. 1983; Abu-Hejleh et al. 1996; Consoli 2000). Thickening of mine tailings via water extraction is an alternative tailings management option that can reduce consolidation settlement and increase water reclamation for reuse in mining operations (Blight 2003; Bussière 2007). However, consolidation of tailings remains a relevant challenge for mine planners and owners as consolidation affects stability and storage capacity of TSFs.

Gibson et al. (1967) presented a governing equation for one-dimensional (1-D) large-strain consolidation of saturated clays and other fine-grained soils that undergo considerable volumetric deformation. The model developed by Gibson et al. (1967) accounts for changes in soil

compressibility and hydraulic conductivity during deformation, which addresses the constraint of small-strain deformation (i.e., constant material properties) in Terzaghi's consolidation theory (Terzaghi 1925). Considerable research has been conducted on large-strain consolidation model formulation (e.g., Koppula 1970; Somogyi 1980; Pane et al. 1981; Znidarcic et al. 1984; McVay 1986; Abu-Hejleh 1996; Fox and Berles 1997) and laboratory evaluation of compressibility and hydraulic conductivity constitutive relationships (e.g., Aubertin et al. 1996; Estepho 2014; Priestly 2011; Suthaker and Scott D. 1996, Znidarcic et al. 1992; Znidarcic et al. 2011). Additionally, large-strain consolidation computer programs have been developed and adopted in mining practice for one-, two-, and three-dimensional (1-D, 2-D, and 3-D) consolidation that can aid TSF design (e.g., Gjerapic 2008; Fredlund and Gitirana 2009; Coffin 2010). Although, large-strain consolidation has been studied extensively since the late 1960s, there are limited full-scale TSF case studies that have been evaluated to document performance of large-strain consolidation models. Furthermore, there has been limited application of 1-D consolidation models, which are more prevalent in practice, to estimate volumetric storage capacity in full-scale TSFs.

The objective of this study was to evaluate performance of commercially-available 1-D large-strain consolidation programs in predicting tailings consolidation to estimate storage capacity of a TSF. Two computer programs (FSConsol and CONDES0) were used to complete the following tasks: (i) assess model applicability via simulating theoretical tailings deposition (instantaneous versus gradual) in a 1-D column; (ii) conduct a parametric study to evaluate the influence of constitutive relationships, initial void ratio, impoundment geometry, and production rate on consolidation behavior; and (iii) predict consolidation and storage capacity of a full-scale copper TSF.

CHAPTER 2: BACKGROUND

2.1 Engineering Characteristics of Mine Tailings

Engineering characteristics of mine tailings discharged into a given TSF are required to predict consolidation behavior. In general, mine tailings can be differentiated into the following categories based on engineering characteristics and consolidation behavior: (i) hard rock, (ii) oil sands, and (iii) phosphate. Hard rock tailings generally exhibit more rapid consolidation when compared to finer tailings such as oil sands and phosphate tailings due to their higher hydraulic conductivity. Hard-rock mining is associated with production of lead, zinc, copper, gold, silver, molybdenum, and nickel (Vick 1983; James 2004), and hard-rock mine tailings typically are composed of sand- and silt-sized particles that exhibit low plasticity to non-plastic behavior (Vick 1983). Oil sands and phosphate mine tailings have negligible sand fractions and considerable clay content such that the type and abundance of clay minerals govern sedimentation and consolidation behavior (BGC Engineering 2010; Carrier et al. 1983; Jeeravipoolvarn et al. 2009; Vick 1983). Research conducted in this study primarily was focused on tailings from hard-rock mines, with particular emphasis on copper tailings due to the case study evaluated.

2.1.1 Geotechnical Characteristics

Geotechnical characteristics of mine tailings that affect consolidation include particle size distribution (PSD), mineralogy, specific gravity (G_s), and plasticity, all of which depend on composition of the ore body and/or the ore milling and extraction process (i.e., method used to liberate minerals for recovery). For example, hard rock tailings often contain “clay-sized” particles resulting from the ore crushing and milling processes as opposed to actual clay minerals. The fine-grained fraction of hard-rock tailings typically is non-plastic and has less influence on the

behavior of mine tailings relative to the presence of actual clay minerals (Vick 1983; Dimitrova 2011.)

Bussière (2007) presented PSDs of nine tailings from different Canadian hard-rock mines prior to deposition in a TSF. The particle diameter at 10 % passing (D_{10}) ranged between 0.001 and 0.004 mm and particle diameter at 60 % passing (D_{60}) ranged between 0.015 and 0.05 mm. The coefficient of uniformity ($C_u = D_{60}/D_{10}$) for these tailings ranged from 8 to 18 and clay content (particles < 0.002 mm in diameter) ranged from 5 to 14 %. Atterberg limits for hard rock tailings exhibit low plasticity index (PI) with a liquid limit (w_L) typically below 40 % and plastic limit (w_P) between 0 and 15 % (Bussière 2007). The general soil classification for hard-rock mine tailings based on the Unified Soil Classification System (USCS) is sandy silt with low plasticity (ML) (Bussière 2007). Specific gravity of hard-rock tailings can range between 2.6 and 4.5 due to variability in parent rock mineralogy (Dimitrova 2011.)

2.1.2 Tailings Solid Content

Solids content (C_p) is defined as the mass of tailings solids per total mass of tailings, which includes solid mass and fluid mass. Tailings discharged from an ore concentrator and tailings discharged into a TSF can have different C_p and engineering characteristics due to mechanical dewatering processes. Mine tailings generally are classified in four groups according to C_p, level of dewatering, or densification (Bussière 2007): (i) conventional tailings, C_p = 30 % to 45 %; (ii) thickened tailings, C_p = 50 % to 70 %; (iii) paste tailings, C_p = 70 % to 85 %; and (iv) filtered tailings, C_p > 85 %.

Conventional tailings are the immediate by-product discharged from an ore concentrator. In water-strained environments (e.g., arid and semi-arid climates), conventional tailings can be dewatered prior to deposition in a TSF to enhance water conservation. Thickened tailings are generated via dewatering in mechanical thickeners. Ideally, thickened tailings are a non-segregating material when deposited in a TSF. Paste tailings are similar to thickened tailings

except a higher degree of thickening and water recovery is achieved. Paste tailings do not segregate and yield minimal water for subsequent recovery following discharge into a TSF. Filtered tailings contain the lowest water content at deposition, which results in a more homogeneous deposit and a reduced land area requirement. Operational costs increase with increasing tailings dewatering (Bussière 2007); thus, dewatering processes are based on site-specific conditions and high-levels of dewatering are not common in large TSF operations.

Mine tailings that are hydraulically pumped to a TSF usually require C_p ranging between 30 % and 60 % (Henderson 1999). Presently, the majority of large, hard-rock mining operations are inclined to operate with $C_p \geq 50$ % by means of thickening technologies with the aim to reuse water for mineral processing (Wels and Robertson 2003; Bussiere 2007). For example, the Escondida mine located in the Atacama desert of Chile manages the Laguna Seca tailings facility with an average discharge rate to the TSF of 240,000 mtpd at $C_p = 50$ % (Chambers et al. 2003.)

2.1.3 Tailings Behavior Within a Storage Facility

Conventional mine tailings discharged into a TSF will experience segregation, sedimentation, and consolidation (Imai 1981; Priscu 1999). Coarser and finer particle fractions of a given mine tailings will segregate following disposal, whereby coarser particles settle in proximity to a discharge point and finer particles are carried in suspension to distal regions of a TSF. Particle segregation liberates water from tailings that collects in a supernatant pond located down-gradient from a discharge point. The supernatant pond also includes water discharged from consolidation of underlying tailings (Priscu 1999).

The coarser tailings fraction deposited proximal to a tailings discharge point forms a beach slope. This slope extends from the discharge point to the supernatant pond and is an important characteristic in TSF design that affects estimates of impoundment capacity. For most types of tailings, beach slopes vary from 0.5 % to 2 % within the first several hundred meters from a

discharge location. Higher beach slope angles are associated with denser (i.e., higher solids contents) and/or coarser tailings (Vick 1983).

The behavior of fine-grained tailings particles in a TSF is analogous to formation of a natural fine-grained soil deposit (Schiffman 1988). Genesis of a natural soil includes three primary stages: flocculation, settling, and consolidation (Imai 1981). Flocculants, which are aggregates of fine-grained particles held together via electro-chemical bonding (Mitchell 1976; Palomino and Santamarina 2005), form during the flocculation stage and subsequently settle out of suspension during the settling stage. Sediment accumulates at the lowest point in a given TSF to create a soil layer, which defines the transition from a slurry material to a soil that has effective stress. As sediment accumulation continues with time, the soil formation line, defined as the point within a sedimenting layer at which effective stress becomes non-zero, increases in height (Imai 1981). Ultimately, all fine-grained tailings particles settle out of suspension, and as effective stress is established throughout the soil layer, consolidation will become the dominant process governing volume reduction of the tailings.

In the consolidation stage, all sediment will experience self-weight consolidation as well as consolidation from induced stress following subsequent tailings deposition. In fine-grained waste disposal, sedimentation is completed within several days as compared to consolidation, which can last several years (Abu-Hejleh 1996; Znidarcic 1999). Therefore, in practice, consolidation of fine-grained mine tailings typically is the only process analyzed (Znidarcic 1999). A critical soil parameter for evaluating consolidation behavior is the initial void ratio at which effective stress becomes non-zero (i.e., void ratio at which settling particles form a soil deposit). Constitutive relationships between (i) void ratio and effective stress and (ii) hydraulic conductivity and void ratio govern consolidation behavior.

2.2 Consolidation Theory

Consolidation is a time-dependent process that involves discharge of water from void space of saturated soils to yield volumetric deformation (Terzaghi 1925; Taylor 1948). Conventional, one-dimensional consolidation theory developed by Terzaghi (1925) was formulated on the assumption that only small strains are achieved, which implies constant permeability and compressibility parameters during consolidation. Slurry materials (e.g., mine tailings) exhibit large-strain deformations following development of effective stress, and deviate from the small-strain assumption in that soil properties continuously change with accumulating deformation (Abu-Hejleh et al. 1996; Caldwell et al. 1984; Carrier et al. 1983; Fox and Berles 1997; Koppula 1970). Thus, large-strain consolidation theories have been developed and numerical models have successfully been applied to settlement behavior of slurry materials (e.g., mine tailings, river sediments, and dredged materials).

2.2.1 Coordinate Systems

Coordinate systems useful in describing the consolidation process are Eulerian and Lagrangian and are shown schematically in Fig. 2.1. The governing equation in small-strain consolidation includes Eulerian coordinates (*x, t*), whereas the governing equation in large-strain consolidation includes Lagrangian coordinates (*a, t*) (Schiffman et al. 1988). The Eulerian coordinate system incorporates a fixed volume in space at a defined distance *x* from a prescribed datum through which both fluid and solids move (Fig. 2.1a). During consolidation, the magnitude and variation of fluid and soil properties (e.g., pore water pressure and void ratio) are observed within the defined volume.

The Lagrangian coordinate system, as applied to consolidation, incorporates a fixed mass of solid particles that defines spatial volume with fluid able to move freely into and out of the volume (Fig. 2.1b). Thus, if the solid mass is in motion, the corresponding spatial volume moves with the solid mass such that the position relative to a prescribed datum changes. Prior to any

consolidation (i.e., soil movement), the initial element ($P_0Q_0R_0S_0$ in Fig. 2.1b) has a Lagrangian coordinate *a* to define location relative to a datum. After consolidation, the initial element has moved and deformed to a new position and element size, as shown by PQRS in Fig. 2b. The new element is at a distance ξ from the datum, is a function of *a* and time *t*, and is called the convective coordinate. During subaerial deposition of slurry materials, the volume of solids in a pre-defined layer does not change, and thus, the solids coordinate (*z*) has been introduced by Gibson et al. (1967) to define the total volume per unit area of solids between the datum plane and a point being analyzed. Schiffman et al. (1988) stated that *z* is adequate for cases where sediment accumulation into a soil layer occurs by a known deposition rate, and the advantage is that by knowing the volume of solids, the consolidation during sediment accumulation can be calculated.

2.2.2 Small-Strain Consolidation Theory

Small-strain consolidation theory developed by Terzaghi (1925) continues to be relevant in many geotechnical engineering problems. The following assumptions are included in the theory: homogeneous soil, complete saturation, negligible compressibility of soil and water, small strains (i.e., hydraulic conductivity and coefficient of compressibility remain constant throughout the consolidation process), 1-D compression, 1-D flow, and Darcy's law is valid. Incorporating these assumptions, Terzaghi proposed the following equation for 1-D dissipation of excess pore water pressure (u_e):

$$c_v \frac{\partial^2 u_e}{\partial x^2} = \frac{\partial u_e}{\partial t} \tag{2.1}$$

where *x* is distance measured downward from the surface of a consolidating soil layer, *t* is elapsed time, and c_v is the coefficient of consolidation. The coefficient of consolidation is defined as

$$c_v = \frac{k(1+e)}{a_v \gamma_w} \tag{2.2}$$

where k is hydraulic conductivity, e is void ratio, a_v is coefficient of compressibility ($a_v = -\Delta e/\Delta\sigma'$, where σ' = effective stress), and γ_w is unit weight of water.

The small-strain assumption in Terzaghi's theory implies constant a_v and k during consolidation (Holtz and Kovacs 1981). The assumption of small strain is not applicable to fine-grained slurries that typically experience considerable change in void ratio during consolidation. These changes in void ratio result in corresponding temporal changes in compressibility and hydraulic conductivity throughout the consolidation process.

2.2.3 Large-Strain Consolidation Theory

Large-strain consolidation models have been developed to overcome the small-strain constraint of Terzaghi´s 1-D consolidation theory. Gibson et al. (1967) used vertical equilibrium, equations of continuity for the solid and fluid phases, and a fluid flow relationship (Darcy's law) to develop a 1-D consolidation theory that accounts for variation in soil compressibility and hydraulic conductivity during consolidation. Gibson et al.'s theory includes a non-linear formulation for self-weight consolidation of saturated, fine-grained soils developed in a Lagrangian coordinate system (Schiffman et al. 1988). The governing non-linear equation in terms of void ratio (e) has the following form:

$$\pm\left(\frac{\rho_s}{\rho_f}-1\right)\frac{d}{de}\left[\frac{k(e)}{1+e}\right]\frac{\partial e}{\partial z}+\frac{\partial}{\partial z}\left[\frac{k(e)}{\rho_f(1+e)}\frac{d\sigma'}{de}\frac{\partial e}{\partial z}\right]+\frac{\partial e}{\partial t}=0 \qquad (2.3)$$

where ρ_s = solid particle density, ρ_f = fluid density, k(e) = hydraulic conductivity as a function of e, and z = solids coordinate that represents volume of solids in a prism of unit cross-sectional area between the datum plane and point of interest at time t (Fig. 2.2).

Gibson et al. (1967) included the following assumptions in development of their theoretical model: (i) the soil skeleton is homogeneous and possesses no intrinsic time effects; (ii) the pore fluid and soil solids are incompressible; and (iii) the principle of effective stress is valid (i.e., σ' =

σ – *u*, where *u* = pore fluid pressure). Priscu (1999) summarized numerous self-weight consolidation applications and accompanying mathematical formulations (i.e., finite-strain formulation or incremental small-strain formulation) as well as the numerical techniques applied in each case. Priscu (1999) reported that essentially all large-strain consolidation models were based on the original formulation presented in Gibson et al. (1967).

Koppula (1970) manipulated the original equation derived by Gibson et al. (1967) to yield the following expression:

$$\frac{\partial}{\partial z}\left[-\frac{k}{\gamma_w(1+e)}\frac{\partial u_e}{\partial z}\right]+\frac{de}{d\sigma'}\frac{\partial \sigma'}{\partial t}=0 \tag{2.4}$$

where u_e = excess pore-water pressure. Somogyi (1980) defined the time variation of effective stress as,

$$\frac{\partial \sigma'}{\partial t}=\left(G_s-1\right)\gamma_w\frac{d\Delta z}{dt}-\frac{\partial u_e}{\partial t} \tag{2.5}$$

where G_s =specific gravity of soil solids and Δz = additional volume of solid particles in a continuous deposition (e.g., deposition of consecutive tailings layers). Substituting Eq. (2.5) in Eq. (2.4) yields Eq. 2.6, which is the governing equation for self-weight consolidation of fine-grained soils in terms of u_e (Somogyi 1980).

$$\frac{\partial}{\partial z}\left[-\frac{k}{\gamma_w\left(1+e\right)}\frac{\partial u_e}{\partial z}\right]+\frac{de}{d\sigma'}\left[\left(G_s-1\right)\gamma_w\frac{d(\Delta z)}{dt}-\frac{\partial u_e}{\partial t}\right]=0 \tag{2.6}$$

2.3 Constitutive Relationships

Constitutive relationships required to model large-strain consolidation include the void ratio – effective stress relationship (*e*-σ', also known as compressibility) and hydraulic conductivity – void ratio relationship (*k*-*e*). These non-linear relationships are necessary to relate the coupled effects of increasing σ' on compressibility and hydraulic conductivity to solve the governing equations of large-strain consolidation (e.g., Eqs. 2.3 and 2.6).

Compressibility and hydraulic conductivity constitutive relationships usually are expressed by power functions as shown in Eqs. 2.7 through 2.9 (Somogyi 1980; Liu et al. 1991; Gjerapic et al. 2008):

$$e = A \cdot \sigma'^{B} \tag{2.7}$$

$$e = A\left(\sigma' + Z\right)^{B} \tag{2.8}$$

$$k = C \cdot e^{D} \tag{2.9}$$

where A, B, C, D, and Z are empirical parameters. Eq. 2.8 represents an expanded form of the widely used *e*-σ' power function in Eq. 2.7. The expanded *e*-σ' relationship (Eq. 2.8) has the advantage that void ratio can be defined at zero effective stress. Applying Eq. 2.7 at zero effective stress implies that void ratio is infinite. To avoid this problem when using Eq. 2.7, a fictitious effective stress is assumed at the top of the consolidating layer equal to $(e_0/A)^{1/B}$, where e_o is initial void ratio (Huerta et al. 1988)

Parameters A, B, C, D, and Z in Eqs. 2.8 and 2.9 can be determined via experimental analysis in a seepage induced consolidation test (SICT) (Znidarcic et al. 1992). The parameter Z has units of stress and is used to define *e* at zero effective stress. The SICT test can be used to accurately determine consolidation parameters for effective stresses below 10 kPa (Geier et al. 2011).

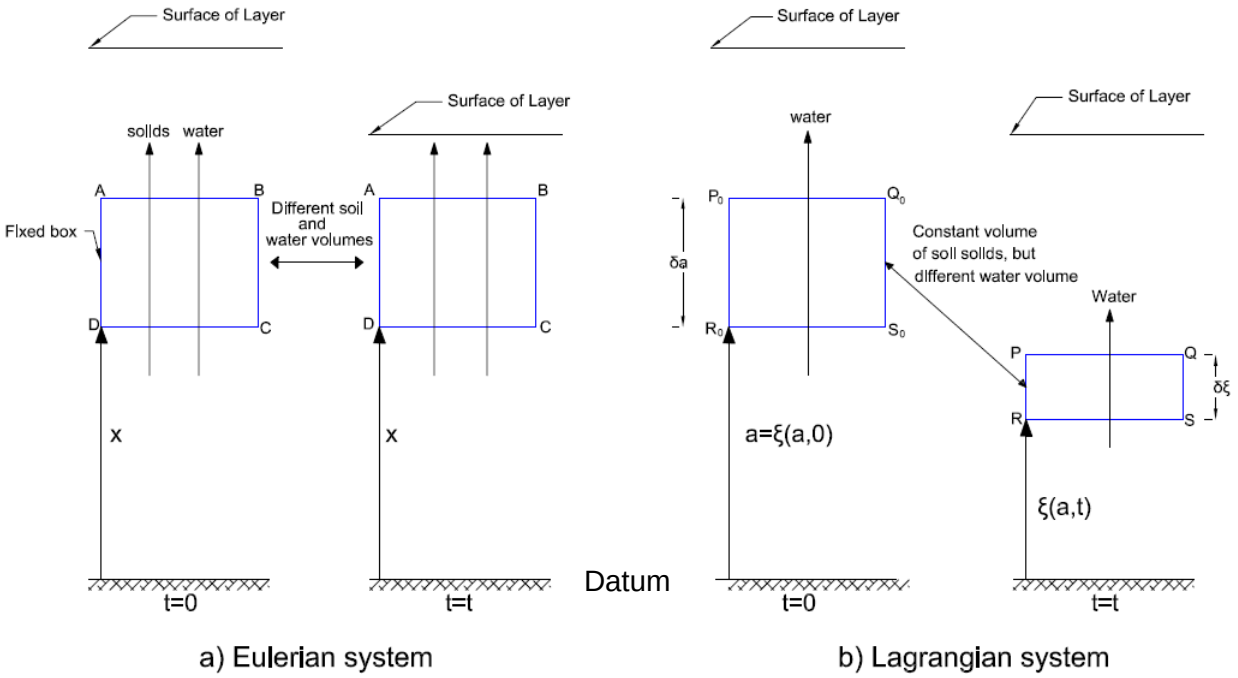

a) Eulerian system b) Lagrangian system

Fig. 2.1. Schematics of Eulerian and Lagrangian coordinate systems from Schiffman et al. (1988). Definitions: x = Eulerian coordinate, distance of fixed element from datum plane, a = initial state Lagrangian coordinate, $\xi(a,t)$ = convective coordinate as function of a and time t, δa = thickness of $P_0Q_0R_0S_0$ element, and $\delta\xi$ = thickness of PQRS element.

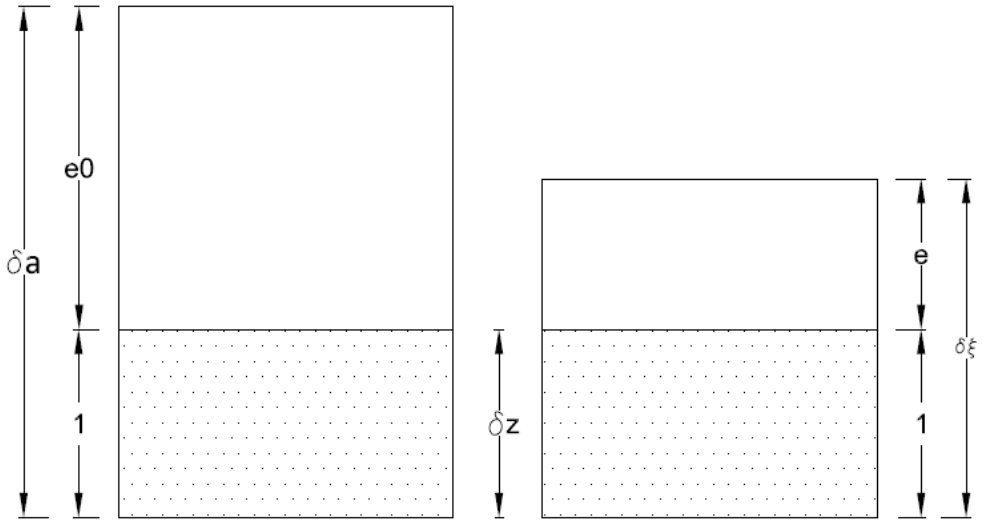

Fig. 2.2. Schematic of coordinate relationships and void ratio change during consolidation from Schiffman et al. (1988). Definitions: z = solids coordinate, e_o = initial void ratio , and ξ = convective coordinate.

CHAPTER 3: MATERIALS AND METHODS

Large-strain consolidation modeling in this study was conducted in three phases: (1) evaluation of benchmark examples; (2) parametric study; and (3) assessment of a full-scale TSF. The benchmark examples were obtained from literature and used to assess functionality of two commercially-available large-strain consolidation computer programs, i.e., FSConsol and CONDES0. The parametric study was conducted to assess the influence of tailings characteristics and design parameters on consolidation behavior. Finally, the full-scale TSF case study was conducted to assess applicability of predicting storage capacity for an actual impoundment facility.

3.1 Mine Tailings

Constitutive parameters for e-σ' (Eq. 2.8) and k-e (Eq. 2.9), e_0, and G_s for mine tailings used in consolidation modeling are summarized in Table 3.1. Constitutive parameters were obtained from the e-σ' and k-e relationships shown in Fig. 3.1. A larger compilation of constitutive relationships for mine tailings was collected during the course of this project and these relationships are included in Appendix A. Copper tailings in Table 3.1 and Fig. 3.1 are from a large-scale open-pit mining operation that incorporates a cyclone station to extract the coarser sand component from the whole tailings. Thus, whole tailings (WT) (Table 3.1) refer to bulk tailings generated at the process plant prior to cycloning. Two whole tailings samples were analyzed: WT-1 represents whole tailings generated during pilot-scale planning for the mine site, and WT-2 represents whole tailings evaluated during full-scale operation of the copper mine. Overflow tailings (OT) refer to the finer-grained material produced from cycloning, which was the primary material discharged into the TSF when the cyclone was operational. These copper tailings

properties were used in consolidation modeling for the case study. Mature fine tailings (MFT), which are predominantly clay-based mine tailings from oil sands production (Estepho 2014), were used in the parametric study to represent a tailings material with different e-σ' and k-e relationships relative to copper tailings.

The WT-2 was classified as CL-ML with D_{10} = 0.002 mm, approximately 60 % fine-grained material (i.e., passing the No. 200 sieve), and G_s = 2.77. In addition, w_L and w_P of WT-2 were 19.8 % and 14.2 %, respectively. Index properties of WT-2 are in agreement with typical values for hard-rock tailings reported in Section 2.1.1. Mature fine tailings from an oil sands operation had approximately 97 % fine-grained content and 89 % clay content (Estepho 2014). Hydraulic conductivity of MFT was approximately three orders of magnitude lower than any fraction of copper tailings (WT or OT) for a comparable void ratio (Fig. 3.1b), which will lead to slower time rates of consolidation.

3.2 Large-Strain Consolidation Models

Commercially-available, 1-D, large-strain consolidation computer programs used in this study included FSConsol v. 3.49 (GWP Geo Software, Edmonton, Alberta, Canada) and CONDES0 (University of Colorado, Boulder, Colorado, USA). These models are capable of simulating deposition and consolidation processes of fine-grained soils that experience large-strain deformation. Both programs include capabilities for impoundment design and planning, and yield output such as settlement versus elapsed time and profiles of average solids content, void ratio, and pore-water pressure at specified elapsed times.

FSConsol is based on the finite-strain consolidation theory in Gibson et al. (1967). The program solves large-strain consolidation with u_e as the independent variable, which is based on the Somogyi (1980) formulation in Eq. 2.6. Although FSConsol is a 1-D model that only simulates vertical drainage and deformation, three-dimensionality of an impoundment can be accounted for via discretizing the impoundment into a number of concentric cylinders as shown in Fig. 3.2 (note:

3rd dimension is into the page). The impoundment filling rate, expressed in terms of dry tailings mass per time, divided by the deposition area is used to determine the filling flux for each concentric cylinder. The compressibility relationship (*e*-σ') used in FSConsol is expressed in the form of Eq. (3.1):

$$e = A \cdot \sigma'^{B} + M \tag{3.1}$$

where A, B, and M parameters are empirical parameters analogous to those in Eqs. 2.7 and 2.8. Also, FSConsol allows inputting a series of points to define the *e*-σ' relationship. FSConsol provides two analyses for conducting large-strain consolidation: (i) tank analysis and (ii) pond analysis. The tank analysis is used to simulate cases in which tailings are added instantaneously and consolidation does not occur prior to complete filling. In the pond analysis, tailings are added gradually and consolidation occurs concurrently with filling.

CONDES0 (CONsolidation and DESiccation) is a finite-difference model capable of simulating 1-D large-strain consolidation and desiccation of fine-grained soils (Yao and Znidarcic 1997). The governing equation in CONDES0 is similar to the 1-D model presented in Gibson et al. (1967) (Yao and Znidarcic 1997; Coffin 2010). CONDES0 employs the expanded power function for the *e*-σ' relationship (Eq. 2.8) and power function (Eq. 2.9) for the *k*-*e* relationship. This program only allows analyzing one type of material, whereas FSConsol has input options for multiple layers with different properties. CONDES0 does not require a deposition area as input, and evaluates 1-D consolidation by neglecting the influence of lateral strains and allowing only vertical flow.

CONDES0 requires a specified filling history for modeling consolidation. This information includes filling stages that encompass the entire period of analysis. For each filling stage, time for the start of filling and end of filling as well as the filling rate need to be specified as illustrated in Fig. 3.3. The schematic in Fig. 3.3 is from the CONDES0 user manual and outlines a recommended tailings deposition sequence. However, in some applications, such as

impoundment capacity estimation during gradual deposition, a pre-defined filling history with beginning and ending times for each stage may not be available.

Coffin (2010) developed a tailings management tool (TMT) to interface with CONDES0. This tool allows consolidation simulations to be conducted for continuous slurry deposition problems by repeatedly using CONDES0 (Miller 2012). The computer interface includes a convenient tab to enter impoundment height-to-surface area pairs and also the production schedule (Fig. A.2), which are typical information provided by mine operations. The TMT developed by Coffin (2010) improves the applicability of CONDES0 to continuous deposition problems. However, this TMT is not commercially-available and was not evaluated in this study.

3.3 Benchmark Examples

Benchmark examples were selected from literature and represent (i) instantaneous deposition of tailings (Townsend and McVay 1990) and (ii) gradual deposition of tailings (Gjerapic et al. 2008). Both examples represent self-weight consolidation of tailings with high initial void ratio and considerable volume change such that large-strain consolidation models are required. Computer programs described in section 3.2 were applied to examples in Townsend and McVay (1990) and Gjerapic et al. (2008) to assess model applicability. Void ratio profiles and temporal trends of surface settlement were obtained from both programs and compared to results from the literature.

3.3.1 Instantaneous Tailings Deposition

A prediction symposium was held in 1987 by the phosphate industry to assess the applicability of numerical models to predict consolidation rates and final consolidation settlement of waste clay disposal ponds (Townsend and McVay 1990). Nine teams of large-strain consolidation modelers evaluated four different waste clay disposal scenarios. The example evaluated in this study included an initial column height of 9.6 m that was assumed

instantaneously filled with phosphate tailings at a uniform e_o = 14.8 and C_p = 16%. Tailings were assumed to consolidate only under self-weight with drainage along the upper boundary and no flow along the bottom boundary and sides of the column.

Constitutive relationships for compressibility and hydraulic conductivity were provided in Townsend and McVay (1990) for phosphate tailings and are shown in Fig. 3.4. Two e-σ' relationships are shown in Fig. 3.4a based on the typical power function (Eq. 2.7) and expanded power function (Eq. 2.8). Select e-σ' data points were identified for the typical power function and then regressed with Eq. 2.8 since parameters for the expanded power function are required input for CONDES0. The typical power function was used in FSConsol with an assumed M = 0.001. The same hydraulic conductivity relationship (Fig. 3.4b) was used in both FSConsol and CONDES0.

The Tank analysis option was selected in FSconsol to model tailings self-weight consolidation. In CONDES0 the selected analysis option was no stage filling (i.e., single, instantaneous filling scenario).

3.3.2 Gradual Tailings Deposition

A schematic of the geometric configuration for the tailings impoundment used in Gjerapic et al. (2008) for gradual tailings deposition is shown in Fig. 3.2a. From this type of impoundment discretization (Fig. 3.2), a relationship between surface height and impoundment surface area was needed to create a height-to-area curve that was used as input when modeling with FSConsol. The geometry of the impoundment modeled was an inverted cone frustum with a base diameter of 300 m, maximum height of 40 m, and side slope of 3.5H:1V. The objective of the model simulation in Gjerapic et al. (2008) was to estimate impoundment capacity by multiplying time required to reach capacity (filling time) by the tailings production rate. A constant tailings

production rate of 2000 mtpd was used in the simulations and filling time was obtained from model output.

The e-σ' and k-e relationships from Gjerapic et al. (2008) are shown in Fig. 3.5. The e-σ' relationship in FSConsol was added as a series of points obtained from the e-σ' curve in Fig. 3.5a. CONDES0 allows entering parameters for the constitutive relationships directly (Fig 3.5a). For both computer programs, the k-e parameters (Fig. 3.5b) were input directly. Also, G_s of tailings was 3.67 and e_o = 5.61, which represents the zero effective stress condition at which large-strain consolidation initiates.

Gjerapic et al. (2008) presented two solutions referred to as lower-bound and upper-bound solutions, which primarily differ in their filling sequence. In the upper-bound solution, impoundment filling is simulated through a series of sequential stacked columns, whereas the lower-bound solution uses concentric annuli of varying heights and areas to represent the impoundment (Coffin 2010). Coffin (2010) noted that the upper-bound solution proposed by Gjerapic et al. (2008) (Fig. 3.2a) uses a similar geometric configuration to that employed by FSConsol (Fig. 3.2b). Therefore, only results from the upper-bound solution from Gjerapic et al. (2008) were compared with results of CONDES0 and FSConsol in this example of gradual tailings deposition. In Fig. 3.2, both geometric configurations are identical when the inter-stage height, f_i, at which the filling rate must change, coincides with the column height, H_i.

In FSConsol, the maximum 40-m height of the inverted cone frustum was sectioned into three 13.33-m-tall columns. This sectioning of the maximum height was arbitrarily defined by Gjerapic et al. (2008) for consolidation modeling. In addition, model simulations with the original tailings impoundment height sectioned into 1–m-tall and 4-m-tall columns were conducted to evaluate the effect of column thickness on consolidation modeling. The 1-m and 4-m column heights were selected for convenience to establish a range in model discretization.

The pond analysis option was selected in FSConsol to model tailings deposition. This option was used to discretize a deposit into various columns or ponds (Fig. 3.2b) by identifying pond area and height, which were obtained from the height versus impoundment surface area curves. Pond area at a specified height and tailings production rate (Q), defined as dry mass of tailings per time, are used in FSConsol to determine filling flux (F). Filling flux is defined as dry mass of tailings per area per time (kg/m^2/d), and is computed for each column to conduct a 1-D consolidation analysis. The model simulation time was defined as 20 yr with F set equal to zero once impoundment capacity was attained. This scenario represents gradual deposition with an initial height of 0 m and a constant Q = 2000 mtpd. The top boundary was defined as free drainage, but, the boundary condition at the bottom of the impoundment was not mentioned in Gjerapic et al. (2008). However, for the simulation in FSConsol completed herein, an impervious bottom boundary was assumed (i.e., bottom boundary = no drainage).

The model simulation in CONDES0 incorporated a drainage boundary at the top, impermeable boundaries along the base and sides, and initial tailings thickness of 0 m. Impoundment filling in CONDES0 is defined as the rate of rise (q) and is in units of length per time. Rate of rise can be calculated as:

$$q_i = \frac{Q}{G_s \rho_w A_i}\left(1 + e_0\right) \tag{3.2}$$

where ρ_w is density of water, e_0 is initial void ratio, A is deposition area, and i identifies the filling stage (Gjerapic et al. 2008). Rates of rise determined for this gradual tailings deposition example are in Table 3.2. Considering three columns, ρ_w = 1000 kg/m^3, G_s = 3.67, and e_0 = 5.61, q decreases as deposition area increases. Filling flux used for FSConsol (Table 3.2) is similar to q used in CONDES0 and can be obtained as the product of q and initial dry density of the tailings.

As discussed previously, pre-defined filling stages are required input for CONDES0 (i.e., filling rates with corresponding durations). However, in the case of continuous tailings deposition, start and end filling times for a given q are not known *a priori*. The following procedure was

implemented to estimate impoundment capacity with CONDES0: Step 1 – divide the deposit into a desired number of columns (three columns was selected for simplicity) and calculate *q* for each column (*q* listed in Table 3.2); Step 2 – conduct independent 1-D consolidation analyses for each column; and Step 3 – sum thicknesses of each independent column to estimate total impoundment thickness and compute capacity. Each independent consolidation analysis starts from time zero and an initial height of zero, and the duration of continuous tailings deposition is such that a given column reaches the specified column height. The time to reach capacity of a given column was fixed and added to subsequent filling time required for the remaining columns to estimate total filling time. One caveat with this independent column analysis in CONDES0 is that consolidation within each column only considers self-weight consolidation of tailings within that column; i.e., weight of tailings in all subsequent columns do not contribute a stress increase to previously analyzed (lower elevation) columns.

3.4 Parametric Study

A parametric study was conducted to examine the effects of four input considerations on large-strain consolidation behavior: (i) constitutive relationships; (ii) initial void ratio; (iii) impoundment geometry; and (iv) tailings production rate. The WT-2 and MFT (Table 3.1) were used to evaluate the effect of constitutive relationships, whereas only WT-2 was used to evaluate effects of the other three input considerations.

The initial void ratio (e_o) identifies density and hydraulic conductivity of a soil deposit at inception of effective stress and affects subsequent changes to *e* and *k* as σ' increases (Znidarcic 1999). Often, e_o is not clearly defined and variation in e_o may influence settlement predictions. Impoundment geometry and tailings production rate are important parameters for a full-scale TSF operation, and variation in these parameters was selected to assess their effects on impoundment capacity and operation life (i.e., filling time)

A 1-D column (pond) with a height of 10 m was used in the constitutive relationship and e_o evaluations, whereas a truncated square pyramid with base width of 100 m and height of 10 m was used to assess impoundment geometry and tailings production rate. A single top-boundary drainage condition was selected for all model simulations.

3.4.1 Constitutive Relationships (e-σ', k-e)

Constitutive relationships are key input parameters that define consolidation settlement and time-rate of consolidation. FSConsol and CONDES0 were employed to assess the influence of different constitutive relationships on consolidation behavior via comparing predictions of settlement, void ratio profiles, and excess pore-water pressure profiles. Oil sand tailings and copper mine tailings were chosen to represent slowly and rapidly consolidating tailings typically encountered in mining practice. The rapidly-consolidating tailings (RCT) was represented by WT-2, whereas slowly-consolidating tailing (SCT) was represented with MFT (Table 3.1; Fig. 3.1).

The impoundment geometry for the constitutive relationship evaluation was defined by a 1-D column. The column was assumed instantaneously filled with tailings at uniform e_o of 5.27 for MFT and 1.71 for WT-2. Boundary conditions for this simulation included no-flow along the base and sides with a single drainage boundary at the top of the column. Excess pore-water pressure is output directly from FSConsol, whereas CONDES0 outputs total pore-water pressure, which includes contributions of static and excess pore-water pressure. Thus, excess pore-water pressure profiles from CONDES0 were created via subtracting static pore-water pressure from output values of total pore-water pressure.

3.4.2 Initial Void Ratio

The evaluation of e_o on consolidation behavior included identical impoundment geometry and boundary conditions as used in the evaluation of constitutive relationships (i.e., 1-D, 10-m tall column; single drainage boundary at top). Tailings were represented by WT-2 and assumed to

be deposited instantaneously with uniform e_o = 1.71 (C_p = 61.8 %). Initial void ratio was altered ± 20 % relative to e_o = 1.71, and the corresponding e-σ' relationships for these tailings are shown in Fig. 3.6. All simulations were conducted assuming self-weight consolidation for a 20-yr time period.

Constitutive relationships for the WT-2 tailings with varying e_o were assumed to have constant A and B parameters; however, Z parameters were calculated to account for variation in e_o (Fig. 3.6). The hydraulic conductivity relationship (Fig. 3.1b) was assumed the same for all three simulations since C and D parameters are defined for a broad range of σ' (Abu-Hejleh et al. 1996), and the effect of e_0 only occurred at low stresses (≤ 10 kPa in Fig. 3.6). FSConsol and CONDES0 were both used to evaluate the effect of e_o on consolidation behavior.

3.4.3 Impoundment Geometry

FSConsol was the only program used to evaluate the effect of impoundment geometry on consolidation behavior. FSConsol is capable of directly simulating gradual tailings deposition problems without a pre-defined filling schedule, whereas CONDES0 requires a pre-defined filling schedule, which in this case was assumed unknown. The pond analysis option of FSConsol was selected for all model simulations with a constant tailings production rate of 100 mtpd and initial height of 0 m. The analysis time allowed for 10 yr of sub-aerial tailings deposition with zero-production rate once impoundment capacity was reached.

Constitutive relationships of WT-2 (Table 3.1) were used for all model simulations. Impoundment geometry was assumed to have the form of an inverted square frustum with 100-m base width and 10-m height as shown in Fig. 3.7. Side slopes of the frustum were varied from 1.0H:1.0V to 4.5H:1.0V. From the specified geometry, height-surface area pairs were calculated for each side slope and then used as input in FSConsol. For example, for an impoundment represented by an inverted square frustum with side slope 1H:1V, the impoundment was divided arbitrary into 0.5 m- increment stages, and for each stage height-area-volume values were

calculated as shown in Fig. 3.7. From these height-area-volume sets, surface area-to-height and volume-to-surface area relationships were created as shown in Fig. 3.8. A single drainage boundary at the surface was selected to allow upward flow of all water discharged during consolidation.

3.4.4 Production Rate

The effect of tailings production rate on consolidation behavior was evaluated considering the same geometric configuration and tailings properties as the impoundment geometry evaluation. Production rates ranged from 50 mtpd to 300 mtpd. This range was selected arbitrarily to examine the effect of decreasing and increasing the production rate relative to simulations completed for the impoundment geometry evaluation (i.e., Q = 100 mtpd). FSConsol was used to conduct all large-strain consolidation analyses. The analysis time was defined for 20 yr of sub-aerial deposition with zero-production rate once impoundment capacity was reached. The simulation time was increased from 10 to 20 yr to all complete impoundment filling for the tailings production rate of 50 mtpd. Simulations were completed for production rates = 50, 100, 200, and 300 mtpd and for each of the side slopes defined in the Impoundment Geometry analyses (i.e., 1.0H:1.0V, 2.0H:1.0V, 2.5H:1.0V, 3.5H:1.0V, and 4.5H:1.0V).

3.5 Case Study

3.5.1 Background

A cross-sectional schematic of the TSF at the full-scale copper mine evaluated in this study is shown in Fig. 3.9. The TSF has been operational for approximately 8 yr and will have a maximum embankment height of 260 m (at centerline) at completion of construction. A rock-fill starter dam was constructed to retain tailings within the TSF and subsequent embankment dam raises were constructed from coarser tailings (underflow) extracted from whole tailings (coarse and fine fractions) via a cyclone. The underflow material predominantly was free-draining coarse

sand, and the remaining fine fraction of the tailings (overflow) was discharged to the TSF for disposal and management. Limited information about the mine has been provided in this report due to proprietary requirements stipulated by the mine owner.

3.5.2 TSF Operation

Ore production and tailings production rates are similar at the copper mine due to the processing of low-grade ores (i.e., low mineral mass percentage contained in the parent rock). The production rate of whole tailings delivered from the thickener at the concentrator plant to the cyclone station initially was 108,000 mtpd based on original design specifications. After approximately three years of operation, ore production increased to 120,000 mtpd due to improvements in the concentration plant. After four years of operation, the annual average coarse fraction recovery (i.e., underflow recovery) at the cyclone station was 32 % for a cyclone operation time (COT) of approximately 70 %. During COT, coarse fraction tailings were separated from whole tailings and used for sequentially raising the tailings dam embankment (Fig. 3.9) and fine fraction tailings were discharged to the TSF. During periods when the cyclone was non-operational, whole tailings were directly discharged into the impoundment.

3.5.3 Available Field Data

Operation data from the copper mine were provided for the first 4 yr, and consisted of monthly average measurements of whole tailings production rates, COT, tailings underflow production, impoundment height, and impoundment volume. Two additional years of data were provided for impoundment height and impoundment volume. Also, a relationship of height-to-surface area of the impoundment geometry was provided, from which a height-to-volume relationship was derived (relationships not included due to proprietary requirements). The latter relationship was developed based on a topographic map of the impoundment and surface areas determined at each height with the assistance of AutoCAD. These height-to-surface area and

height-to-volume relationships were used to estimate tailings dry density within the TSF. The procedure for creating these height-surface area-volume relationships is similar to the example presented in Section 3.4.3.

Topographic surveys periodically were conducted that consisted of surveying the tailings surface elevation and depth of the supernatant pond. These surveys, combined with ground topography and mass of tailings discharged to the impoundment, were used to compute an average dry density of the impounded tailings.

3.5.4 Consolidation Modeling

Consolidation behavior of the full-scale copper TSF was predicted using FSConsol to estimate impoundment height and tailings dry density. CONDES0 is not directly applicable for estimating impoundment capacity or filling times since a pre-defined production schedule is required for model simulation. Also, CONDES0 only allows input for a single set of constitutive relationships that represents one tailings, and due to varying COT in that actual operation, tailings discharged into the TSF varied temporally. On the other hand, FSConsol includes the option to evaluate multiple materials and is suitable for calculating capacity based on tailings mass. Therefore, modeling of the impoundment case study only was conducted with FSConsol.

The height-to-surface area relationship of the impoundment geometry mentioned in Section 3.5.3 was discretized in a number of 5-m-tall columns to not exceed the maximum number of columns (80 columns) in FSConsol. The impoundment consisted of *n* one-dimensional columns with corresponding surface areas A_i (i = 1, 2, …,n) and impoundment heights H_i (i = 1, 2, …,n) from the bottom to the top of each column, where H_0 = 0. These A_i and H_i pairs were input into FSConsol to discretize the actual impoundment. The maximum height of the impoundment was set at H_n = 253 m (Fig. 3.10).

Two large-strain consolidation simulations were conducted with FSConsol: (i) Design Assessment and (ii) Operation Assessment. A summary of the tailings production schedule and percentages of discharged overflow and whole tailings for the Design Assessment at COT of 70 % and 90 % is in Tables 3.3 and 3.4, and for the Operation Assessment at COT of 70 % and 90 % is in Tables 3.5 and 3.6. The Design Assessment incorporated initial design criteria of production rate and underflow recovery (Tables 3.3 and 3.4), whereas the Operation Assessment included annual average tailings production rates, COT, and underflow recovery for the first four years of operation (Tables 3.5 and 3.6). Weighted average G_s and C_p for tailings discharged to the impoundment are included for the Operation Assessment to reflect actual tailings within the TSF.

In the Design Assessment, tailings production rate was assumed to increase linearly during the first six months of operation (ram-up period), which was followed by a constant production rate of 108,000 mtpd for the remainder of TSF operation. Underflow recovery was assumed to be 34 % to reflect initial design specifications, and COTs of 70 % and 90 % were considered. These COTs were selected to bound the 85 % COT specified in the original design criteria and average COT of 70 % based on the first 4 yr of operation.

The Operation Assessment included annual average tailings production, COT, and underflow recoveries for the first 4 yr of operation (Tables 3.5 and 3.6). For all subsequent years, a production rate of 120,000 mtpd, average underflow recovery of 34 %, and COT of either 70 % (Table 3.5) or 90 % (Table 3.6) were considered. Also, constitutive relationships for WT-2 (i.e., tailings evaluated after two years of operation) were incorporated in the analysis to more appropriately reflect actual operation conditions. The WT-1 was evaluated from pilot design, whereas WT-2 was evaluated during design and were coarser relative to the gradation of WT-1. However, similar consolidation parameters of OT (Table 3.1) were used during all periods because the revised gradation (after two years of operation) was comparable with gradation used during design.

Production schedules used in the Design and Operation assessments are included in Tables 3.3 through and 3.6. In these tables, the tailings discharge rate to the impoundment is the actual rate used for modeling with FSConsol. The overflow and whole tailings categories are percentage contributions to the actual tailings productions rates.

3.5.5 Tailings Characteristics

Whole tailings produced at the concentrator plant generally classified as clayey silt with low plasticity index (5.6) and $w_L \approx 20$. The reported G_s was 2.77. These index parameters are in agreement with general geotechnical characteristics for tailings described in Section 2.1.1. Also, only a fraction of total generated tailings were deposited into the TSF. The actual amount of tailings discharged into the impoundment depends on the COT and underflow recovery (UF), which represents the amount of coarser tailings extracted from whole tailings. Thus, tailings discharged into the impoundment during full-scale operation (Q^*) was calculated from Eq. 3.3.

$$Q^* = Q\left(1 - COT \cdot UF\right) \tag{3.3}$$

Contributions of overflow (%OT) and whole tailings (%WT) in the bulk composition of the tailings discharged to the TSF were calculated from Eqs. 3.4 and 3.5.

$$\%OT = \frac{\left(COT - COT \cdot UF\right)}{1 - COT \cdot UF} \tag{3.4}$$

$$\%WT = 100 - \%OT \tag{3.5}$$

Percentages of overflow and whole tailings for different COTs are presented in Tables 3.3 through 3.6. For example, in Table 3.5, average tailings production in Year 1 was 73,218 mtpd and the rate of tailings discharged to the impoundment was 60,047 mtpd from which 55 % was overflow

and 45 % whole tailings (i.e., tailings from concentrator plant directly discharged to the impoundment).

Individual *e*-σ*'* and *k*-*e* constitutive relationships for tailings discharged to the TSF in the Design and Operation Assessments are shown in Figs. 3.11 and 3.12. Due to assumptions of COT in the Design assessment and differences in COT and UF in the Operation Assessment, unique *e*-σ' and *k*-*e* constitutive relationships were needed for the impounded tailings to more effectively capture consolidation behavior. All modified constitutive relationships were calculated using a weighted average technique based on the portion of OT and WT that constituted tailings discharged to the TSF. A weighted average technique was applied to individual *e*-σ' and *k*-*e* data points obtained from consolidation data provide by the mine engineers. A similar weighted average procedure was used to estimate G_s and e_o of the impounded tailings.

3.5.6 Modeling Output and Assessment

Average ρ_d of tailings within the copper mine TSF was estimated by two different procedures (Procedure 1 and Procedure 2) as shown in Fig. 3.13. These techniques were compared to actual tailings ρ_d in the TSF obtained from the mine records. The objective of the ρ_d estimation evaluation was to determine a practical and appropriate technique to translate 1-D model results from FSConsol to estimations of ρ_d in a full-scale TSF.

In Procedure 1, average ρ_d was computed directly from the average C_p output from FSConsol (Fig. 3.13). Complete saturation of tailings within the TSF was assumed and ρ_d at a given time *t* was calculated based on Eq. 3.6.

$$\rho_d(t) = \frac{G_s \rho_w}{1 + \left(\frac{1}{C_p(t)} - 1 \right) G_s} \tag{3.6}$$

The total impoundment volume (V_t) corresponding to ρ_d from Eq. 3.6 was calculated as:

$$V_t = \frac{M_s}{\rho_d} \tag{3.7}$$

where M_s is dry mass of tailings discharged into the TSF, which was obtained from FSConsol at the same t corresponding to calculations of ρ_d and V_t. Temporal calculations of V_t were compared to the calculated maximum volumetric capacity of the impoundment, based on actual geometry of the facility, to estimate the operational life (i.e., filling time). Finally, impoundment height was calculated as the tailings height attained for a calculated V_t based on the height-to-volume relationship derived for the impoundment geometry. The horizontal surface of tailings was assumed perfectly flat (i.e., no beach slope) to relate tailings height to impoundment volume.

In Procedure 2, the total impoundment volume (V_t) was first estimated from surface height (H_t) generated from FSConsol and the height-to-volume relationship of the actual impoundment geometry. Average ρ_d was then computed as the quotient of M_s deposited into the TSF and V_t for a given time t. The time required to reach the maximum V_t was taken as the operational life.

Calculation methodologies in Procedure 1 and Procedure 2 both used cumulative mass of solids discharged into the impoundment (M_s), which were obtained for select times as output from FSConsol. The total predicted impoundment capacity in dry tailings mass was assumed equal to M_s from FSConsol output at the time corresponding to complete filling of the TSF (i.e., end of operational life of the TSF). Alternatively, impoundment capacity can be estimated as the product of a constant filling rate and the estimated operational life. In this full-scale case study, filling rates varied with time due to different COT's and underflow recoveries (Tables 3.3-3.6). Thus, impoundment capacity can be estimated as the sum of the product of each filling rate multiplied by the corresponding duration until the operational life is reached.

Table 3.1. Consolidation constitutive parameters (e-σ', k-e), initial void ratio (e_o), and specific gravity (G_s) for mine tailings used in numerical analyses.

Location	Material [a]	Name	e_0 [b]	G_s	A	B	Z (kPa)	C (m/s)	D	Reference
Parametric and case studies	Cu whole tailings	WT-2	1.71	2.77	1.3	-0.168	0.192	1.02E-07	3.42	Case study: actual operation
Case study	Cu whole tailings	WT-1	1.29	2.73	1.03	-0.115	0.141	1.55E-07	2.80	Case study: pilot plan
Case study	Cu overflow tailings	OT	3.21	2.725	1.67	-0.127	0.006	4.62E-08	3.06	Case study: pilot plan
Parametric study	OS tailings	MFT	5.26	2.65	3.52	-0.236	0.181	1.10E-11	3.79	Estepho (2014)

Note: *A, B, C, D and Z* = material parameters determined from laboratory measurements or curve fitting

[a] Cu, copper ; OS, oil sand

[b] Initial void ratio, $e_0=A.Z^B$

Constitutive relationships : $e = A\,(\sigma' + Z)^B$ and $k = Ce^D$

Table 3.2. Column height, surface area, rate of rise, and filling flux used for model simulations in FSConsol and CONDES0 for the benchmark example in Gjerapic et al. (2008). Impoundment geometry was discretized into three columns and represented by an inverted cone frustum with base diameter of 300 m, maximum height of 40 m, and slide slope of 3.5H:1V.

Column No.	Base elevation of each column (m)	Surface area of each column (m^2)	*q* (m/day)	*F* (kg/day-m^2)
1	0.00	70,690	0.0510	28.293
2	13.33	121,500	0.0297	16.461
3	26.67	186,000	0.0194	10.753

Note: *q* = Rate of rise; F = filling flux

Table 3.3. Tailings production rate schedule and percent contributions of overflow and whole tailings to discharged tailings at the full-scale copper tailings impoundment used in the Design assessment with 70 % COT.

Period		Tailings production rate[a]	Tailings discharge rate to impoundment[b]	Overflow[c]	Whole tailings[d]
Year	Month	(mtpd)	(mtpd)	(%)	(%)
1	1	12,000	9,144	61	39
1	2	31,200	23,774	61	39
1	3	50,400	38,405	61	39
1	4	69,600	53,035	61	39
1	5	88,800	67,666	61	39
1	6-12	108,000	82,296	61	39
2 to end	All	108,000	82,296	61	39

[a] Linear ramp-up during the first six month, and then tailings production of 108,000 mtpd

[b] Amount of tailings deposited into the impoundment

[c] Percentage contribution of overflow to tailings deposited into the impoundment, 70 % COT and 34% underflow recovery

[d] Percentage contribution of whole tailings to tailings deposited into the impoundment

Table 3.4. Tailings production rate schedule and percent contributions of overflow and whole tailings to discharged tailings at the full-scale copper tailings impoundment used in the Design assessment with 90 % COT.

Period		Production rate[a]	Tailings discharge rate to impoundment[b]	Overflow[c]	Whole tailings[d]
Year	Month	(mtpd)	(mtpd)	(%)	(%)
1	1	12,000	8,328	86	14
1	2	31,200	21,653	86	14
1	3	50,400	34,978	86	14
1	4	69,600	48,302	86	14
1	5	88,800	61,627	86	14
1	6-12	108,000	74,952	86	14
2 to end	All	108,000	74,952	86	14

[a] Linear ramp-up during the first six month, and then tailings production of 108,000 mtpd.

[b] Amount of tailings deposited into the impoundment.

[c] Percentage contribution of overflow to tailings deposited into the impoundment, 90 % COT and 34% underflow recovery.

[d] Percentage contribution of whole tailings to tailings deposited into the impoundment.

Table 3.5. Tailings production rate, cyclone operation time, underflow recovery, percent contributions of overflow and whole tailings in discharged tailings into the impoundment, and weighted average specific gravity and solids content of copper tailings used in the Operation Assessment.

Year	Production rate [a] (mtpd)	COT [b] (%)	Underflow recovery [c] (%)	Tailings discharge rate to impoundment (mtpd)	Overflow (%)	Whole tailings (%)	Weighted average G_s	Weighted average C_{p0} (%)
1	73,218	63	29	60,047	55	45	2.75	53
2	103,333	79	38	72,516	70	30	2.74	51
3	100,668	57	30	83,410	48	52	2.75	54
4	106,274	81	30	80,491	74	26	2.74	50
5 to end	120,000	70	34	91,440	61	39	2.74	52

[a] Years 1 to 4 = average annual production rates; Year 5 to end of operation = 120,000 mtpd (assumed)

[b] Years 1 to 4 = average annual cyclone operation times (COT); Year 5 to end of operation, COT = 70 % (assumed)

[c] Years 1 to 4 = average annual underflow recovery; Year 5 to end of operation = 34% (assumed)

Table 3.6. Tailings production rate, cyclone operation time, underflow recovery, percent contributions of overflow and whole tailings in discharged tailings into the impoundment, and weighted average specific gravity and solids content of copper tailings used in the Operation Assessment.

Year	Production rate [a] (mtpd)	COT [b] (%)	Underflow recovery [c] (%)	Tailings discharge rate to impoundment (mtpd)	Overflow (%)	Whole tailings (%)	Weighted average G_s	Weighted average C_{p0} (%)
1	73,218	63	29	60,047	55	45	2.75	53
2	103,333	79	38	72,516	70	30	2.74	51
3	100,668	57	30	83,410	48	52	2.75	54
4	106,274	81	30	80,491	74	26	2.74	50
5-End	120,000	90	34	83,280	86	14	2.73	48

[a] Years 1 to 4 = average annual production rates; Year 5 to end of operation = 120,000 mtpd (assumed)

[b] Years 1 to 4 = average annual cyclone operation times (COT); Year 5 to end of operation, COT = 90 % (assumed)

[c] Years 1 to 4 = average annual underflow recovery; Year 5 to end of operation = 34% (assumed)

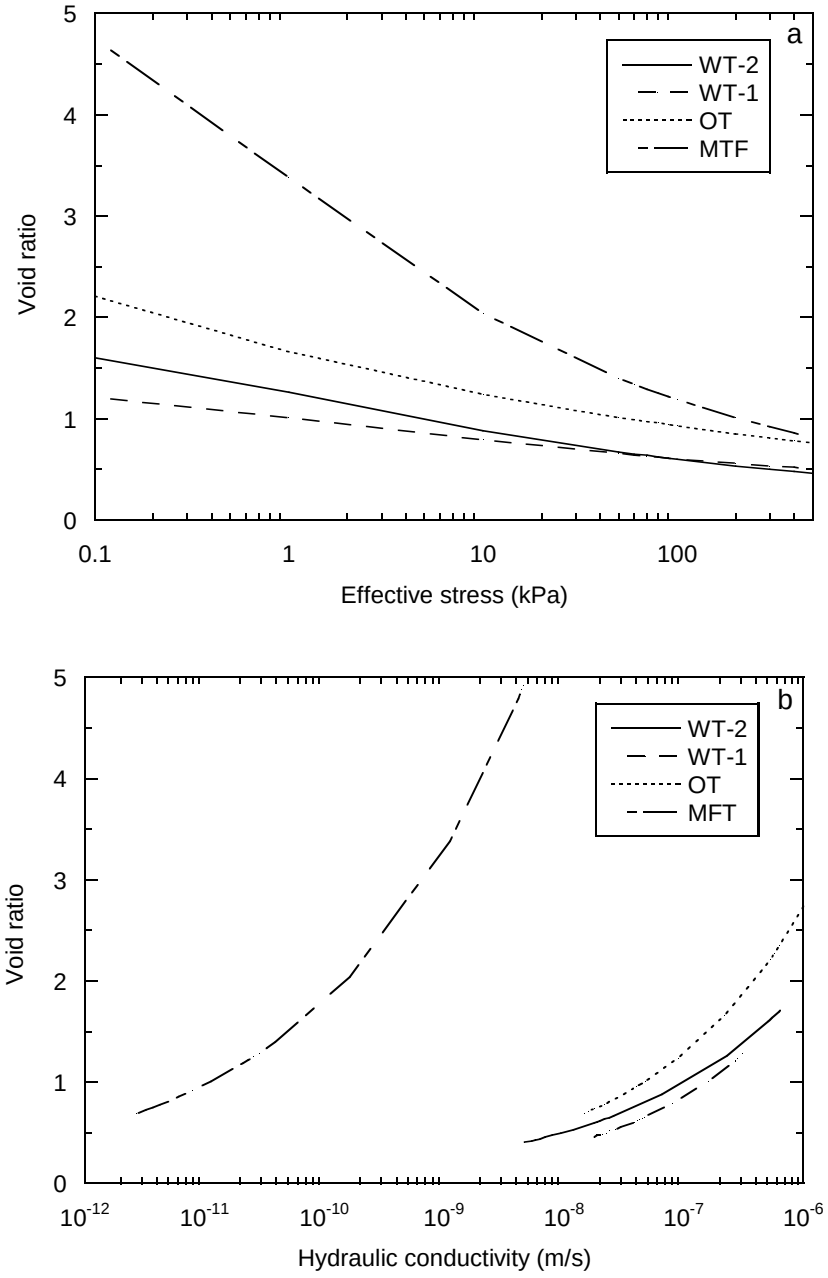

Fig. 3.1. Constitutive relationships for mine tailings used in the parametric study and case study: (a) effective stress versus void ratio relationships and (b) void ratio versus hydraulic conductivity relationship. Note: WT-1 = copper whole tailings from pilot-scale evaluation, WT-2 = copper whole tailings from full-scale operation, OT = copper overflow tailings, and MFT = oil sand mature fine tailings.

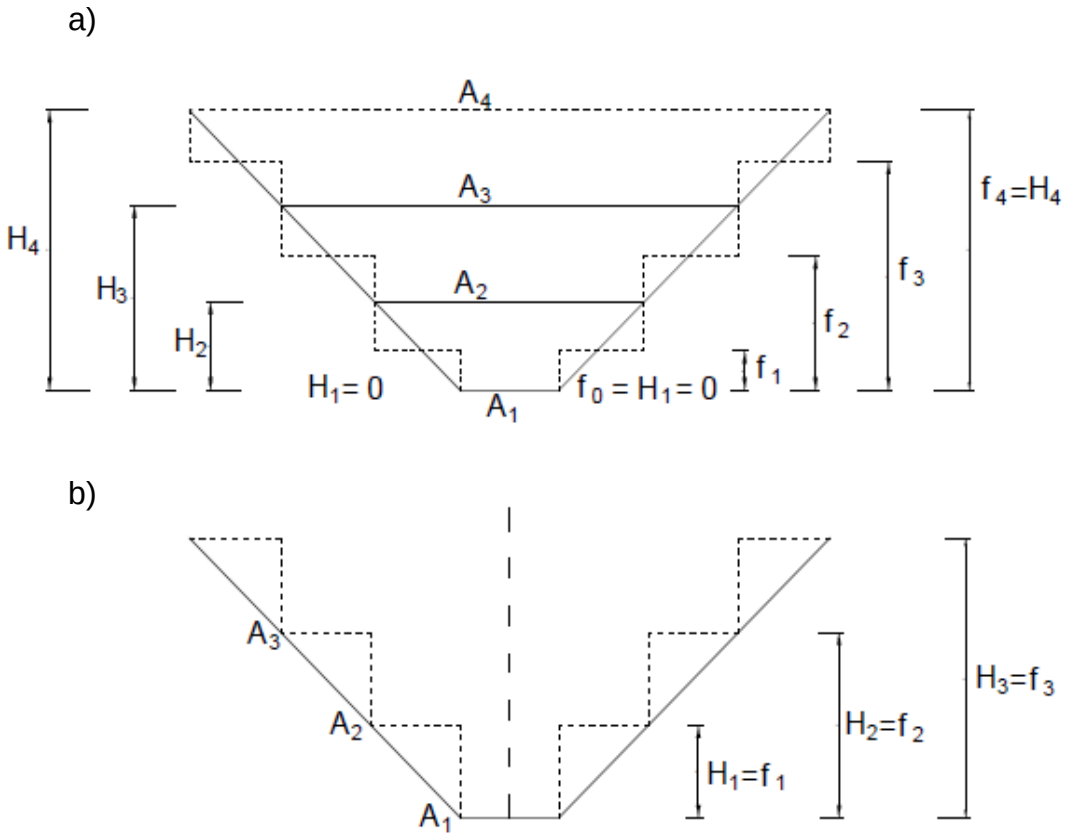

Fig. 3.2. Geometrical discretization schemes of (a) a tailings impoundment assuming four filling stages (upper bound solution in Gjerapic et al. 2008) and (b) general configuration assumed in FSConsol (figures from Coffin 2010): Note: H_i = column height, f_i = inter-stage heights at which the filling rate changes, and A_i = deposition area for each column.

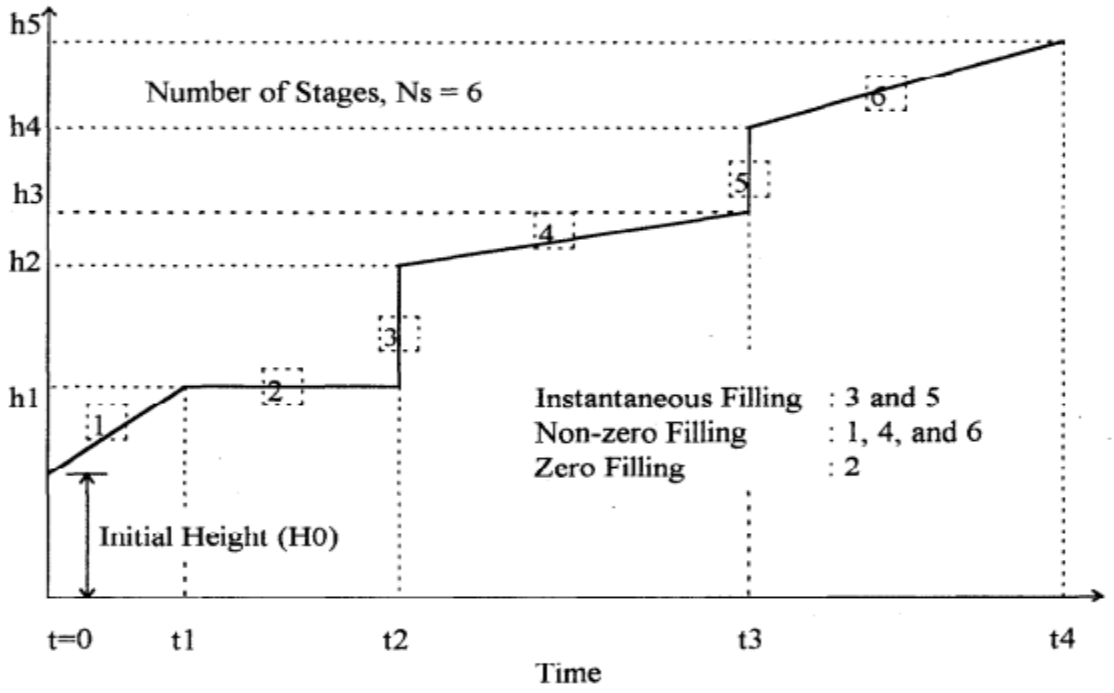

Stage number	TBF	TEF	FRH	Filling Type
1	0	t1	(h1-H)/t1	Non-zero Filling
2	t1	t2	0	Zero Filling
3	t2	t2	(h2-h1)	Instantaneous Filling
4	t2	t3	(h3-h2))/(t3-t2)	Non-zero Filling
5	t3	t3	(h4-h3)	Instantaneous Filling
6	t3	t4	(h5-h4)/(t4-t3)	Non-zero Filling

Fig. 3.3. Deposition chart of nominal height versus time and input table for staged filling used in CONDES0 (Yao and Znidarcic 1997).

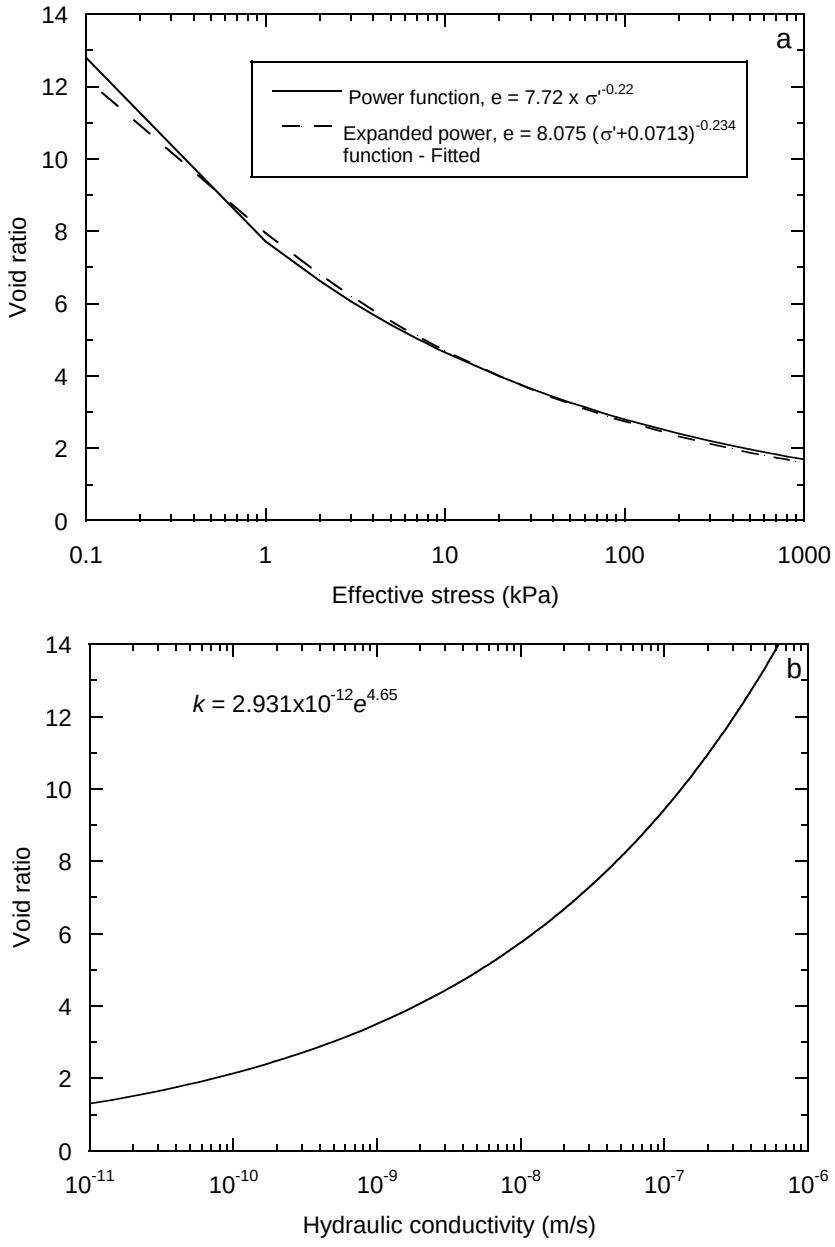

Fig. 3.4. Constitutive relationships from Townsend and McVay (1990) used in the instantaneous tailings deposition benchmark example: (a) effective stress versus void ratio relationship with power function based on Eq. 2.7 and expanded power function based on Eq. 2.8, and (b) hydraulic conductivity versus void ratio relationship with power function relationship based on Eq. 2.9.

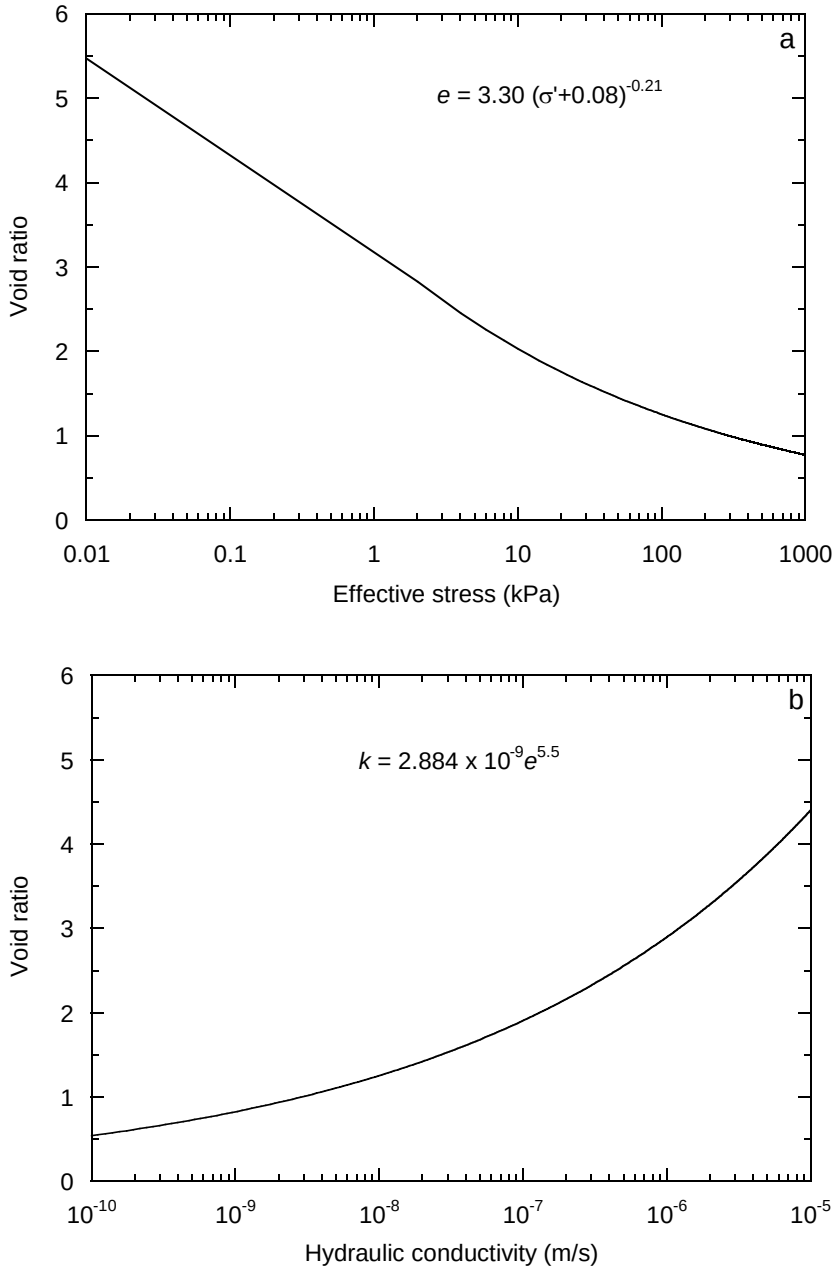

Fig. 3.5. Constitutive relationships from Gjerapic et al. (2008) used in the gradual tailings deposition benchmark example: (a) effective stress versus void ratio and (b) hydraulic conductivity versus void ratio.

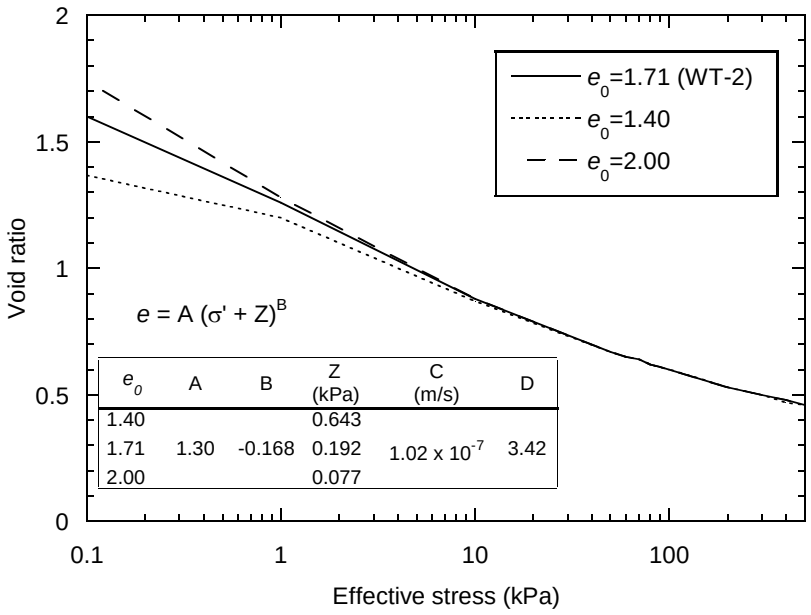

Fig. 3.6. Effective stress versus void ratio relationships of copper tailings (WT-2, Table 3.1) for initial void ratios (e_0) of 1.4 (- 20 %), 1.71 (base case), and 2.0 (+ 20 %).

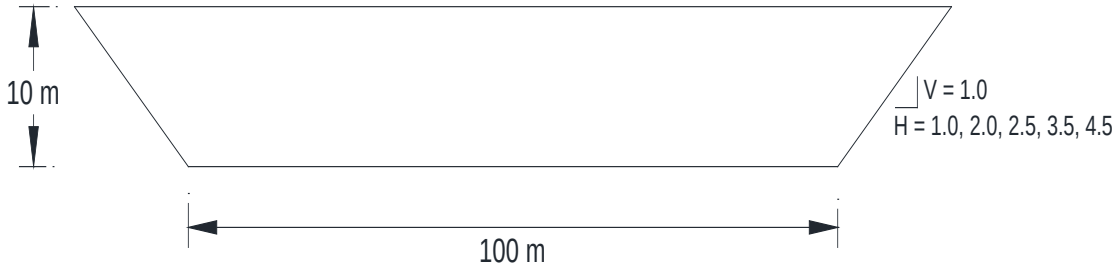

Stage	Height m	Area m^2	Volume m^3
1	0.5	10,201	5,050
2	1.0	10,404	10,201
3	1.5	10,609	15,455
4	2.0	10,816	20,811
5	2.5	11,025	26,271
6	3.0	11,236	31,836
7	3.5	11,449	37,507
8	4.0	11,664	43,285
9	4.5	11,881	49,172
10	5.0	12,100	55,167
11	5.5	12,321	61,272
12	6.0	12,544	67,488
13	6.5	12,769	73,816
14	7.0	12,996	80,257
15	7.5	13,225	86,813
16	8.0	13,456	93,483
17	8.5	13,689	100,269
18	9.0	13,924	107,172
19	9.5	14,161	114,193
20	10.0	14,400	121,333

Fig. 3.7. Typical cross-section of inverted square frustum for the five different side slopes, H (horizontal = 1.0, 2.0, 2.5, 3.5. and 4.5) and V (vertical = 1) evaluated in this study, and tabulation of impoundment height – surface Area – volume relationship for an inverted frustum with side slope 1H:1V.

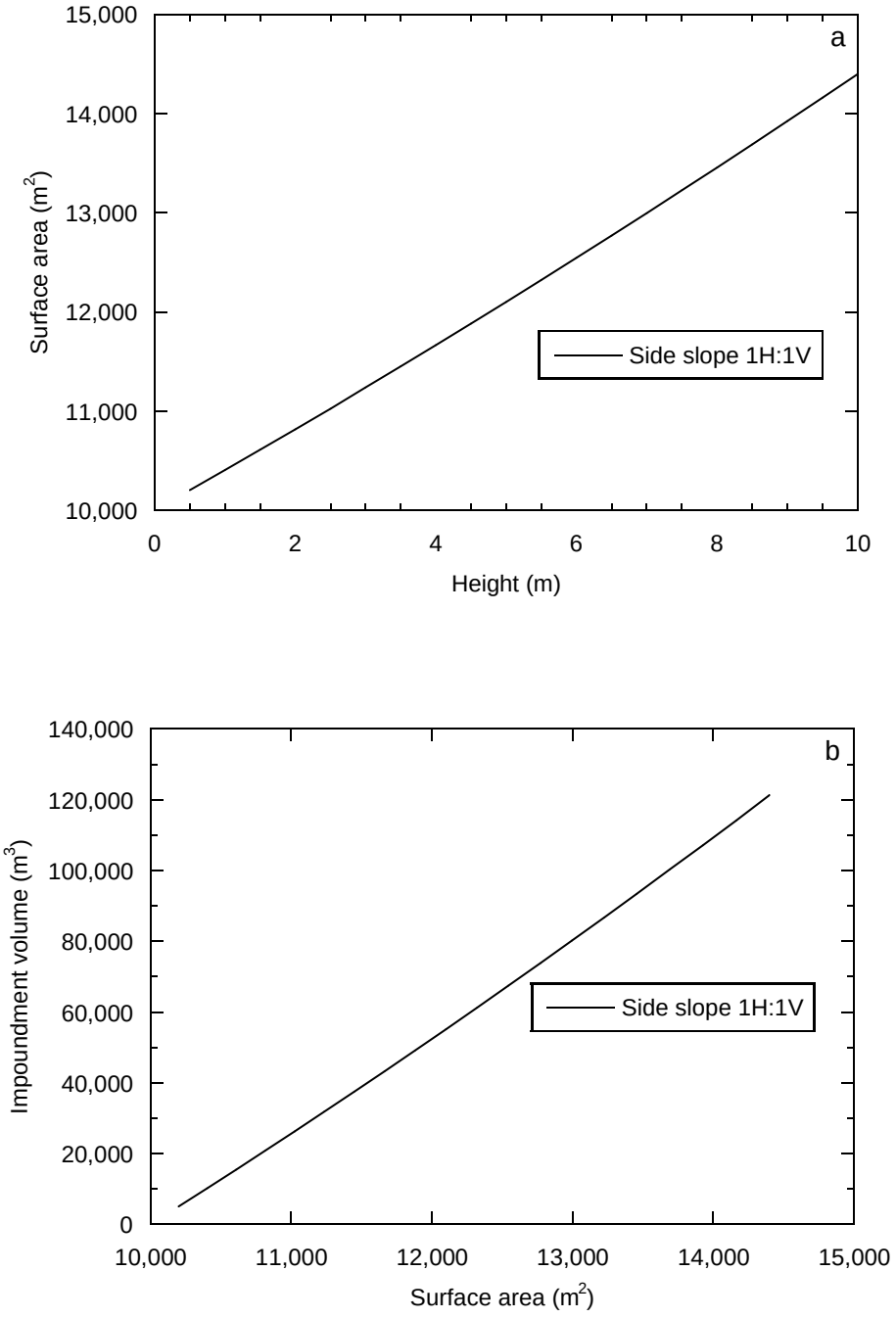

Fig. 3.8. Impoundment surface area versus height relationship (a) and impoundment volume versus surface area relationship for an inverted square frustum with 1H:1V side slopes.

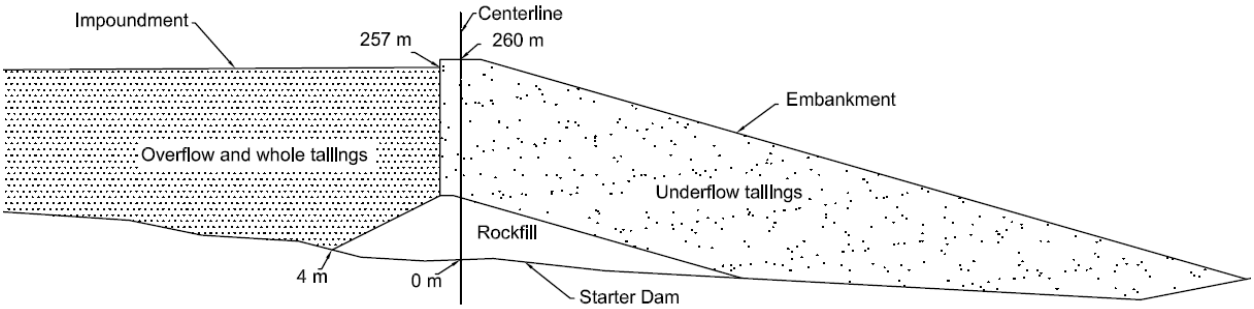

Fig. 3.9. Typical cross-section of the centerline embankment dam for the full-scale tailings storage facility case study; maximum embankment height = 260 m (at centerline) and maximum tailings impoundment height = 253 m. The impoundment contains overflow tailings, which are the finer fraction after cycloning, and whole tailings, which are bulk tailings discharged directly from the concentrator plant without cycloning. The embankment is built from the coarse fraction after cycloning (underflow tailings).

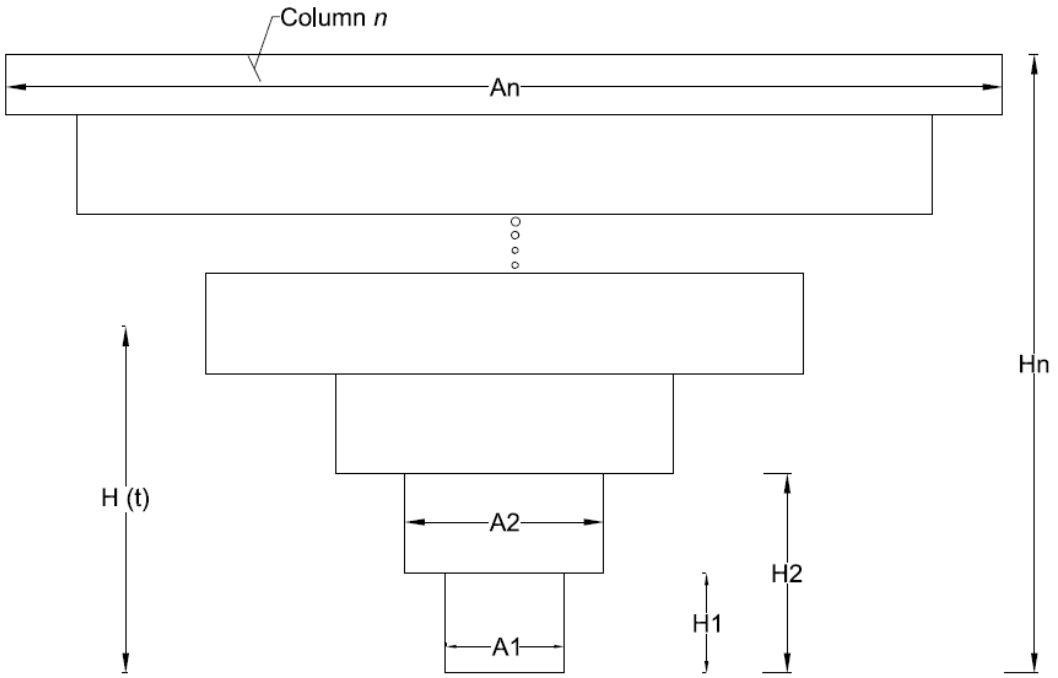

Fig. 3.10. Geometrical discretization of the full-scale copper tailings impoundment for the numerical simulations. Notes: $H_{(t)}$ tailings surface height at time *t;* H_i, A_i are column height and surface area of column *i*, respectively.

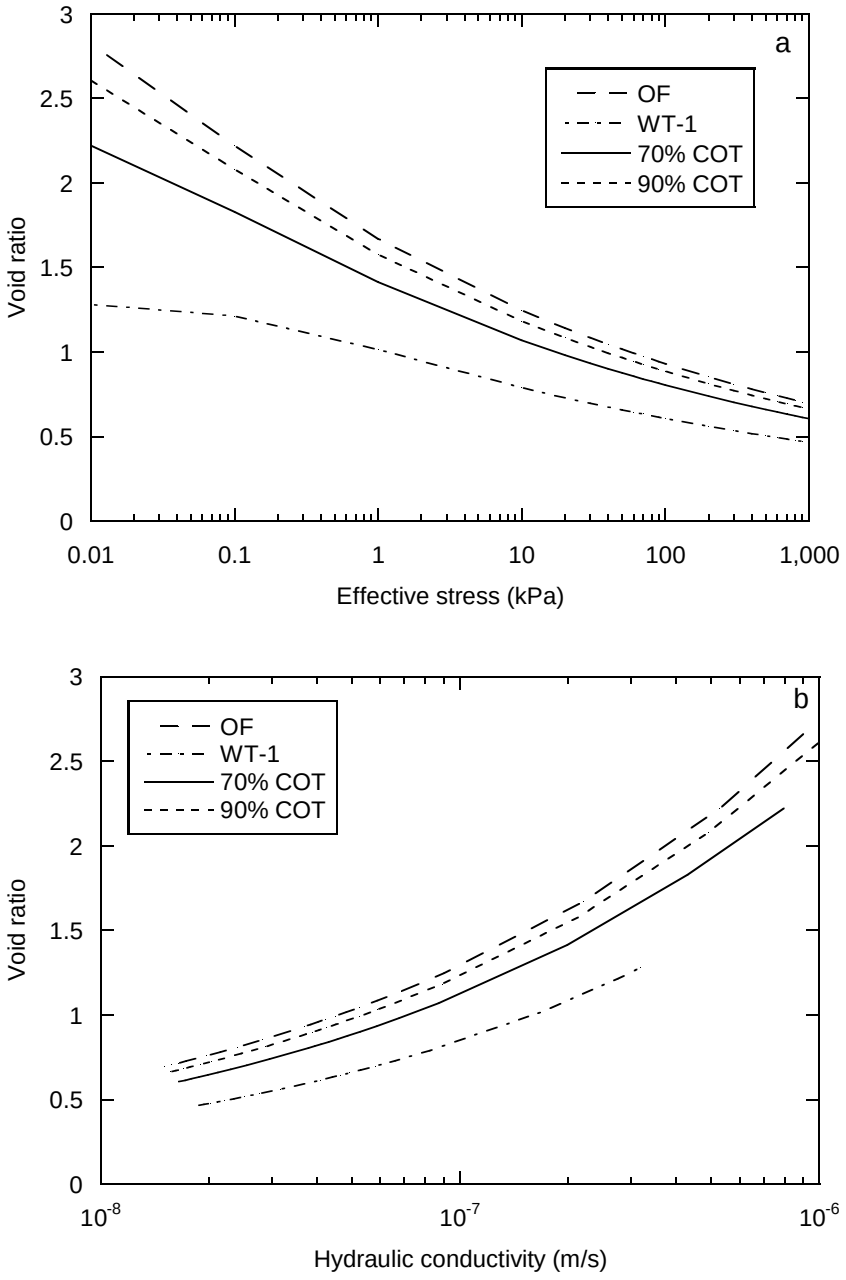

Fig. 3.11. Constitutive relationships for impounded tailings used in the Design Assessment with 70 and 90 % cyclone operation time (COT) assumed during the entire operation life of the facility: (a) effective stress versus void ratio and (b) hydraulic conductivity versus void ratio. Relationships computed by using a weighted average of OF and WT-1 are labeled as 70% COT and 90% COT curves.

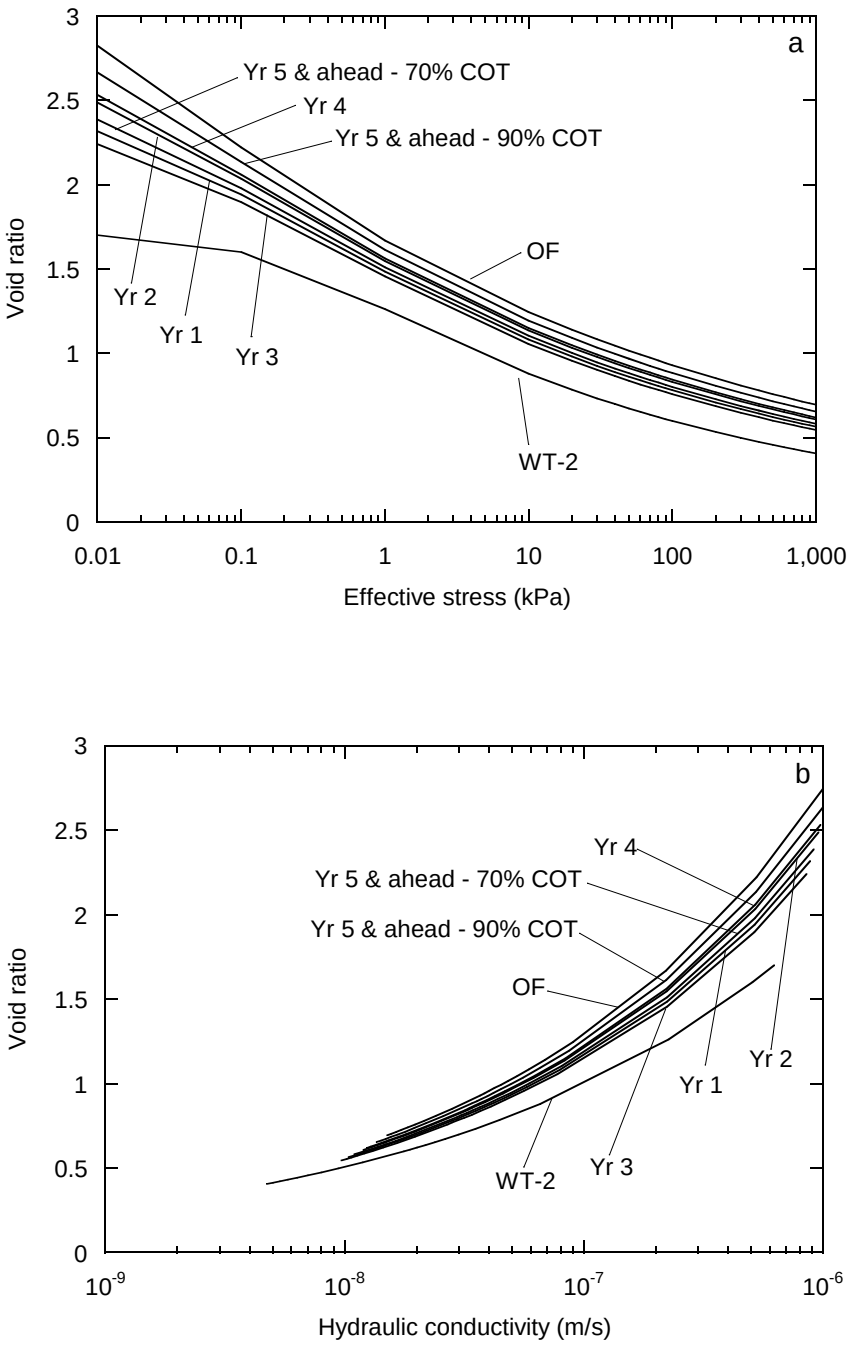

Fig. 3.12. Constitutive relationships for impounded tailings used in the Operation Assessment with 70 and 90 % COT assumed for Year 5 to the end of operation: (a) effective stress versus void ratio and (b) hydraulic conductivity - void ratio. All curves, with exception of OF and WT-2, were used in the models and developed from a weighted average of OF and WT-2.

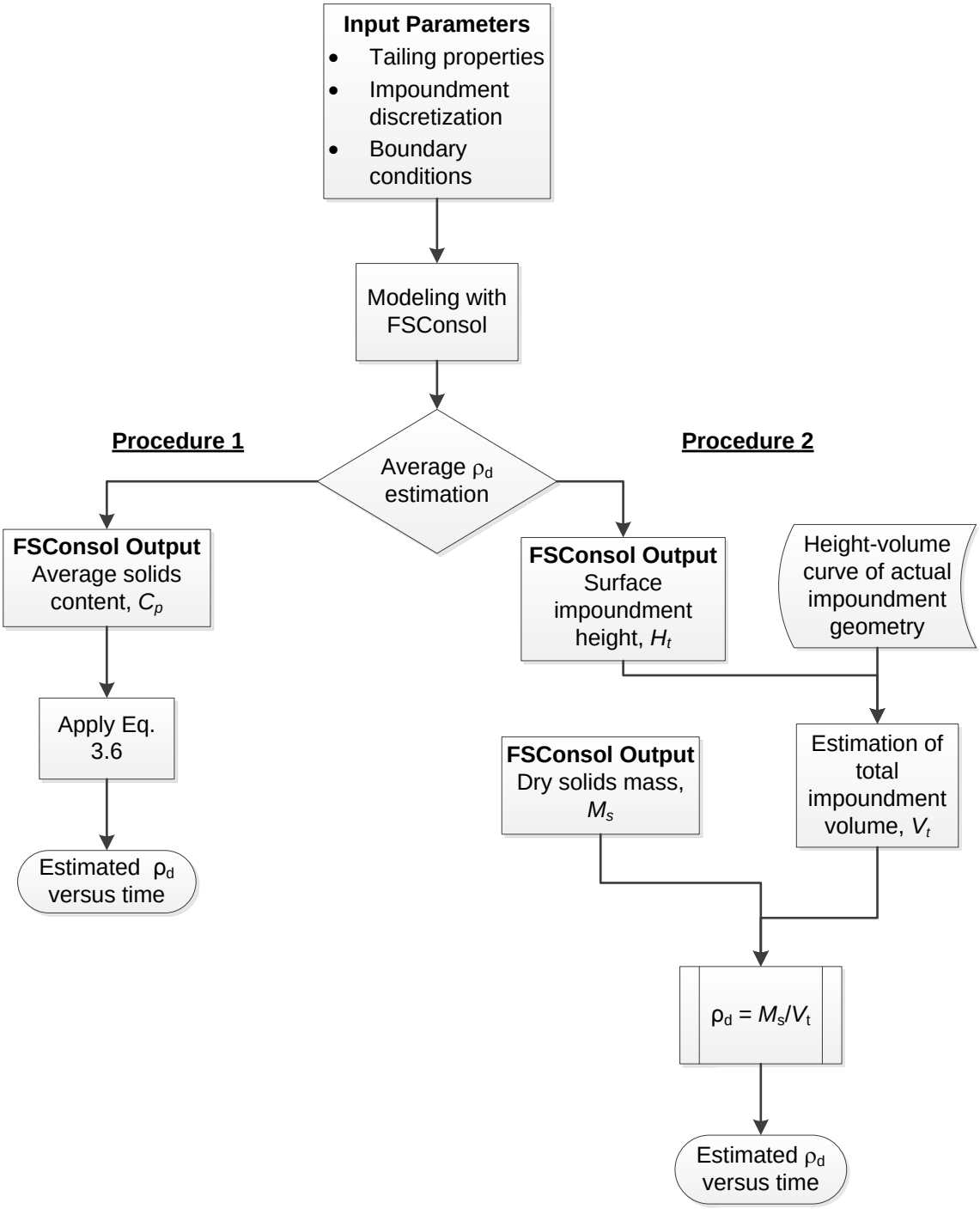

Fig. 3.13. Flow chart of dry density estimation techniques, Procedure1 and Procedure 2, based on FSConsol output and actual height-volume relationship of the full-scale tailings storage facility.

CHAPTER 4: RESULTS AND DISCUSSION

4.1 Benchmark Examples for Consolidation Modeling

4.1.1 Instantaneous Tailings Deposition

A summary of 1-D large-strain consolidation results that include the average results from the nine modeling teams summarized in Townsend and McVay (1990), FSConsol, and CONDES0 are in Table 4.1. These consolidation results include final tailings height, tailings height at 1 yr, and void ratio at the base of the tailings layer at 1 yr. The nine modeling teams in Townsend and McVay (1990) generated twelve different settlement predictions and ten void ratio profile predictions. At the end of Year 1, the tailings height was 7.19 m with a standard deviation (SD) of 0.42 m for predictions in Townsend and McVay (1990), and the final tailings height and SD reduced to 4.16 ± 0.05 m. The final height from the simulation conducted in CONDES0 was 4.18 m and in FSConsol was 4.13 m, which are similar to the average final tailings height of 4.16 m from predictions in Townsend and McVay (1990). Additionally, all predictions yielded good agreement for void ratio at the base of the column at the end of Year 1 (Table 4.2).

Temporal trends of tailings height (i.e., settlement) for model simulations presented in Townsend and McVay (1990) as well as simulations with FSConsol and CONDES0 are shown in Fig 4.1a. Nearly 85 % of total predicted settlement occurred within the first 1000 d (2.7 yr) for all model simulations. A final, approximately constant tailings height was achieved by 4000 d (~ 11 yr) in all model simulations (Fig. 4.1a).

CONDES0 and FSConsol yielded similar settlement predictions that also were comparable to most simulations compiled in Townsend and McVay (1990). Three predictions compiled from Townsend and McVay (1990) (B&CI, UCONN, and A&Assoc as identified in Fig. 4.1) exhibit minor deviation from the general settlement trends shown in the other models. These predictions underestimated settlement between approximately 10 and 500 d (Fig. 4.1a), but ultimately converge with all model predictions to a final impoundment height (Table 4.1).

Profiles of void ratio at the end of 1 yr of consolidation modeling are shown in Fig. 4.1b. In general, a decreasing void-ratio profile is shown for all model simulations, which is in agreement with relatively rapid consolidation occurring during the first year (Fig. 4.1a). Void ratio profiles in Fig. 4.1b can be differentiated into two general relationships. The first relationship is a continuously decreasing void ratio with depth, which was predicted by the majority of simulations in Townsend and McVay (1990) as well as with CONDES0 and FSConsol. The second relationship shows a constant void ratio in the upper part of the column (height > 4 m in Fig. 4.1b) and decreasing void ratio at greater depths within the tailings deposit (height < 4 m in Fig. 4.1b). The second void-ratio relationship corresponds to the same three predictions that disagreed with the general settlement trend in Fig. 4.1a (i.e., B&CI, UCONN, and A&Assoc). Higher void ratios from these three predictions were expected due to lower settlement predicted for Year 1.

CONDES0 and FSConsol produced nearly identical predictions of settlement and void ratio, and were consistent with the majority of results compiled from Townsend and McVay (1990). Townsend and McVay (1990) suggested that discrepancies between model predictions were due to input variability since two predictions used similar programs but resulted in different behavior. The minor differences between CONDES0, FSConsol, and remaining 1-D predictions compiled from Townsend and McVay (1990) may be attributed to differences in forms of e-σ' relationships, mesh discretization, time-step, or other features used to solve the governing equations.

4.1.2 Gradual Tailings Deposition

Temporal trends of impoundment height from FSConsol and CONDES0 model simulations of the gradual tailings deposition example in Gjerapic et al. (2008) are shown in Fig. 4.2. Gjerapic (2008) presented two methods referred to as lower-bound and upper-bound solutions. The upper-bound solution in Gjerapic et al. (2008) is used for comparison of impoundment capacity and filling time as this solution accounts for tri-dimensionality of a tailings impoundment without requiring excessive computational effort required in the application of 2-D or 3-D consolidation equations.

The upper-bound solution assumed impoundment filling through a series of sequential stacked columns (Fig. 3.2a), and Coffin (2010) noted that FConsol uses a similar filling simulation (Fig. 3.2b). For this reason, only the upper-solution model was considered in this study.

Filling time and impoundment capacity for the simulations in FSConsol and CONDES0 as well as from the upper-bound solution in Gjerapic et al. (2008) are in Table 4.2. In general, results from Gjerapic et al. (2008) and FSConsol are comparable when impoundment height was discretized into 1-m-thick columns for the FSConsol simulation. However, as column thickness was increased in FSConsol, filling time and total tailings capacity were underestimated (Table 4.2), which was attributed to decreased model resolution with a decreasing number of columns. Thus, accounting for a larger number of columns via model discretization reduced the underestimation of impoundment capacity and filling time (Table 4.2). This observation suggests that good practice is to enhance model discretization via increasing the number of stacked columns (i.e., number of surface area-elevation pairs) in FSConsol such that the total volume of all columns will yield a volume close to the actual impoundment volume to be modeled.

Filling time and impoundment capacity based on CONDES0 were both underpredicted relative to FSConsol simulations and results from Gjerapic et al. (2008) (Table 4.2 and Fig. 4.2). These underpredictions were attributed to lower predictions of tailings settlement. The separation of total impoundment thickness into a number of independently analyzed columns to predict consolidation in CONDES0 for the continuous deposition scenario led to reduced self-weight loading on underlying tailings, which reduced total settlement (Fig. 4.2). Therefore, the commercially-available software CONDES0 may not be the most appropriate model to simulate tailings impoundment capacity during continuous tailings deposition.

4.1.3 Implications of Benchmark Examples

The instantaneous tailings deposition benchmark example from Townsend and McVay (1990) evaluated with CONDES0 and FSConsol indicated that both models are appropriate for

predicting tailings consolidation behavior and determining heights for storage capacity estimates in cases where tailings are deposited instantaneously (i.e., very rapid relative to the duration of the analysis). The gradual tailings deposition benchmark example from Gjerapic et al. (2008) suggested that FSConsol can be readily applied to determine impoundment storage capacity for specified tailings production rates and impoundment geometry. However, gradual tailings deposition could not readily be applied in the commercially-available version of CONDES0. Thus, FSConsol was found more applicable for tailings depositional strategies (i.e., continuous deposition) that are reflective of full-scale TSFs.

4.2 Parametric Study

4.2.1 Constitutive Relationships

One-dimensional large strain consolidation analyses were conducted for a slowly (SCT) and rapidly (RCT) consolidating tailings to evaluate the effects of different constitutive relationships (e-σ', k-e) on consolidation behavior. A comparison of impoundment height predictions based on FSConsol and CONDES0 versus time for SCT and RCT is in Fig. 4.3. FSConsol and CONDES0 yielded nearly identical temporal trends of impoundment height for both tailings evaluated, which suggests that both models simulated consolidation behavior similarly. Predicted impoundment height at 95 % average excess pore-water pressure dissipation for SCT was 5.3 m after a period of approximately 375 yr. In contrast, consolidation in RCT was nearly complete after only 1.6 yr (600 d), which corresponded to a final predicted impoundment height of 6.5 m. The difference in elapsed time for completion of consolidation was due to low hydraulic conductivity of the SCT (i.e., MFT in Fig. 3.1b), which increased time required to dispel excess pore-water pressure. Furthermore, after approximately 100 yr both computer programs predicted similar impoundment heights for SCT (Fig. 4.3), whereas a modest difference (0.27 m) was observed at completion of model simulation (i.e., 500 yr). Negligible differences (~ 0.1 m) were observed at the end of consolidation for RCT (Fig. 4.3).

Profiles of excess pore water pressure (u_e) for RCT and SCT are shown in Fig. 4.4. FSConsol and CONDES0 results of u_e are essentially identical for both the RCT and SCT simulations. Excess pore-water pressure was largest at the base of the simulation for both RCT and SCT, which was modeled as a no-flow boundary, and decreased with increasing elapsed time. Near complete u_e dissipation was achieved in < 2 yr for RCT (Fig. 4.4a), whereas approximately 400 yr was required to achieve near complete u_e dissipation for SCT (Fig. 4.4b). The initial u_e at the base of the simulated column (height = 0 m) for RCT is higher than SCT because RCT had a higher buoyant unit weight that increased u_e during self-weight consolidation.

Void ratio profiles at different elapsed times during consolidation for both FSConsol and CONDES0 simulations are shown in Fig. 4.5. Overall, evolution of the *e*-profiles as a function of time and material were similar in FSConsol and CONDES0. Trends in Fig. 4.5 exhibit typical shapes of self-weight consolidation, whereby a transition from concave to convex profiles develop with increasing elapsed times. Ito and Azam (2013) presented a similar evolution in *e*-profiles for 1-m-tall columns of soils classified as sedimentary clays. Predictions with both models (FSConsol and CONDES0) show a decrease in void ratio with depth due to larger induced vertical stress that also increases the potential for consolidation settlement near the base of the simulation compared to material near the upper boundary (Fig. 4.5)

Void ratios near the end of the simulation were similar between the two programs, which supports the similar predictions of final impoundment height (Fig. 4.3). Both programs appear to be suitable to accommodate differences in tailings characteristics for consolidation analysis. However, void ratios at early times were found sensitive to program inputs such as number of time steps and form of *e*-σ' relationship.

4.2.2 Initial Void Ratio

Temporal relationships of impoundment height for three different values of e_0 for RCT (i.e., WT-2 copper tailings) are shown in Fig. 4.6. Settlement was predicted with FSConsol and

CONDES0 and both programs yielded similar temporal trends of settlement for all three e_0 considerations. For example, FSConsol yielded a final height of 7.38 m for e_o of 1.4, whereas with CONDES0 yielded a final height of 7.30 m. Settlement increased with increasing e_o, and the time required to complete consolidation settlement decreased with increasing e_o.

The increase in predicted settlement (i.e., decrease in impoundment height) with increasing e_o was due to greater initial void volume that coincides with greater settlement potential. A decrease in the initial C_p increased the rate of consolidation due to higher e_o and higher k that decreased time required for dissipation of u_e. For example, average final height of the impoundment (average of outputs from both computer programs) increased from 6.59 m to 7.34 m as e_0 decreased from 1.71 to 1.4. In addition, the average final height increased from 6.02 m to 6.59 m as e_0 decreased from 2.0 to 1.71.

4.2.3 Impoundment Geometry

Predicted filling times and impoundment capacity based on FSConsol (in dry mass) for a theoretical tailings basin with five different side slope configurations are summarized in Table 4.3. An increase in the ratio of horizontal-to-vertical (H:V) dimension (i.e., decrease in side slope angle) increases total available storage volume and results in increased tailings capacity. Filling time increased and rate of rise (q) decreased as H:V increased due to additional time required to reach ultimate capacity for a constant tailings production rate (Table 4.3). The rate of rise represents the rate at which the tailings impoundment increases in height and is a function of production rate, impoundment geometry, and distribution system for sub-aerial deposition (i.e., distribution of discharge points). Low rates of rise (small increases in surface elevation) enhance drainage via shortening the drainage path lengths (i.e., thinner layer) that promote more rapid dissipation of u_e.

Excess pore-water pressure profiles at elapsed time = 5.5 yr for each side slope are shown in Fig. 4.7. With exception of the 1.0H:1.0V side slope, a consistent decrease of u_e was observed

throughout the depth of the simulated impoundment as the side slope H:V ratio increased (Fig. 4.7). At a given height within the impoundment, the increase loading due to subsequent tailings deposition decreased for impoundments with flatter slopes because tailings were distributed across a larger surface area. Therefore, assuming water is relatively incompressible and the bottom boundary of the impoundment is impervious, this low application of load will result in lower u_e. For example, u_e at the base of the impoundment (height = 0 m) for a side slope of 4.5H:1.0V was approximately 2.6 kPa compared to 5.3 kPa for the 2.0H:1.0V case (Fig. 4.7). The lower u_e profile for the 1.0H:1.0V case compared to both the 2.0H:1.0V and 2.5H:1.0V slopes, particularly in lower depths of the tailings deposit, was due to the ultimate capacity of the impoundment with 1.0H:1.0V achieved in 5.2 yr and u_e plots were developed at 5.5 yr (Fig. 4.7 and Table 4.3). Thus, once ultimate capacity is achieved, subsequent increases in u_e will not occur as there is no additional tailings deposition to increase u_e.

The average ρ_d of tailings is an important parameter in the estimation of impoundment capacity (Vick 1983; Cacciuttolo and Barrera 2012), and depends on factors such as TSF geometry, deposition plan, rate of rise, specific gravity of solids, tailings solids content, and tendency of tailings to segregate following deposition (Cacciuttolo and Barrera 2012). Low tailings ρ_d reduces impoundment capacity and increases the volume of water retained within the pore space of the impounded tailings (Barrera 1998). Predicted ρ_d of the impounded tailings after 4 yr of simulation time and at full impoundment capacity are summarized in Table 4.3. Dry density was calculated based on total solid tailings mass discharged to the impoundment (obtained as output from FSConsol) and the simulated TSF volume occupied. There is relatively minor variation in ρ_d as a function of side slope and time (Table 4.3), since the low tailings production rate (i.e., 100 mtpd) and relatively high hydraulic conductivity of the WT-2 tailings yielded comparable magnitudes of u_e dissipation for all side slope cases (Fig. 4.7). The larger ρ_d that correspond to steeper side slope angles (i.e., lower H:V) after 4 yr of deposition were attributed to increased

self-weight loading since the same cumulative dry tailings mass was discharged into a smaller total simulated impoundment volume.

4.2.4 Production Rate

Impoundment filling time and total impoundment capacity (in mass of dry tailings) for tailings production rates ranging between 50 and 300 mtpd and side slopes ranging from 1.0H:1.0V to 4.5H:1.0V are summarized in Table 4.4. Relationships of normalized dry capacity and normalized filling time versus production rate are shown in Fig. 4.8. Dry capacity and filling time were normalized with respect to results for a filling rate of 50 mtpd. As production rate increased, impoundment dry capacity and filling time decreased regardless of impoundment geometry. There was a slight decrease in capacity with increasing production rate for all scenarios (Fig. 4.8a), and the most pronounced decrease in capacity was observed for a side slope of 1.0H:1.0V. For example, impoundment dry capacity for the 1.0H:1.0V side slope configuration decreased from 192,000 Mg to 186,000 Mg as production rate increased from 50 mtpd to 300 mtpd (Table 4.4). This decrease was only 3.1 % relative to capacity for 50 mtpd. Therefore, changes in production rate have limited effect on the impoundment dry capacity for the range of production rates evaluated in this study. In addition, filling times decreased at the same rate that production rates increased regardless of side slope (Fig. 4.8b). Normalized filling time decreased by a factor of 2 for all side slopes when production rate was increased from 50 mtpd to 100 mtpd.

Profiles of u_e at an elapsed time of 1.4 yr for impoundments with side slopes of 1.0H:1.0V and 4.5H:1.0V for tailings production rates ranging between 50 and 300 mtpd are shown in Fig. 4.9. Larger increases in u_e were observed with steeper side slope angles due to higher rates of rise (i.e., greater amount of tailings deposited in a given elapsed time). The variations of u_e shown in Fig. 4.9 suggest that both side slope angle and tailings production rates influence u_e.

Predicted average u_e dissipation during the 20 yr analysis for an impoundment with 1.0H:1V side slopes and the entire range of tailings production rates is shown in Fig 4.10. The

average degree of u_e dissipation on reaching ultimate capacity, identified as the inflection points in Fig. 4.10, increased with decreasing production rate. Considering comparable hydraulic conductivity for all scenarios, lower average u_e dissipation for higher production rates was a direct consequence of longer drainage path lengths due to thicker deposited tailings layers.

4.2.5 Practical Implications of Parametric Study

The implications of the parametric study are relevant for engineers interested in the effect of tailings material parameters and TSF design and operational parameters on the planning and design of TSFs. Determination of reliable constitutive relationships is critical to long-term TSF management (e.g., reclamation initiatives and closure plans) since a decrease in tailings hydraulic conductivity of multiple orders of magnitude can considerably extend the time required for consolidation (Fig. 4.3). Prolonged consolidation time will limit strength gain within the tailings and render tailings non-trafficable, which will limit site reclamation. Also, proper understanding of the constitutive relationships can support the application of technologies to accelerate consolidation to avoid the demand of more and larger TSFs (e.g., wick drains, geotextile bags, physical-chemical treatment of tailings). Similarly, e_o is a parameter that can decrease or increase impoundment capacity (Fig. 4.6), and more precise measurement of e_o will lead to improved estimates of impoundment capacity.

Average ρ_d at the completion of impoundment filling for the range of side slopes evaluated converged to a narrow range of 1.574 Mg/m^3 and 1.581 Mg/m^3 (Table 4.3). Barrera (1998) reported average dry densities of copper tailings ranging from 1.24 Mg/m^3 to 1.38 Mg/m^3 during about the first eight years of operation for six large Chilean deposits with similar G_s. Also, Cacciuttolo (2012) reported final average dry density of 1.30 Mg/m^3 after 10 yr of operation (operation period from 1999 to 2008) at Los Quillayes copper TSF in Chile with similar characteristics to the case study evaluated herein (i.e., G_s = 2.7 and concentrator production rate of 115,000 mtpd). The observed ρ_d in this parametric study combined with field values in Barrera

(1998) and Cacciuttolo (2012) suggests that a maximum average ρ_d may need to be considered for engineering design of TSFs. Subsequent consolidation simulated via numerical modeling will lead to higher ρ_d; however, the viability of these higher ρ_d should be evaluated.

4.3 Full-Scale TSF Case Study

The applicability of FSConsol to predict consolidation of copper mine tailings in a full-scale TSF was evaluated considering a Design assessment and an Operation assessment. The Design assessment accounted for initial criteria used in design of the TSF, whereas the Operation assessment accounted for actual production data and tailings characteristics collected during full-scale operation of the TSF.

4.3.1 Average Dry density

Temporal trends of actual average tailings ρ_d and predictions of average ρ_d for the Design and Operation assessments that consider both Procedures 1 and 2 to compute ρ_d are shown in Fig. 4.11. Comparisons between annual average predicted tailings ρ_d and actual tailings ρ_d are shown graphically in Fig. 4.12. Calculation of ρ_d via Procedure 2 (Fig. 3.13), which is based on impoundment height output from FSConsol, yielded higher ρ_d and better agreement with actual ρ_d when compared to results from Procedure 1 for both the Design and Operation assessments (Figs. 4.11 and 4.12). Additionally, the temporal trends in Fig. 4.11 are shown for COTs of 70 % and 90 %, where the higher COT implies a larger contribution of the finer tailings fraction was assumed discharged to the TSF. In general, a COT of 90% led to lower predicted ρ_d for the Design assessment due to higher void ratios associated with the finer fraction OT for a given level of effective stress (Fig. 3.1a).

A coefficient of determination (R^2) was computed for each of the model simulations shown in Fig. 4.11 and are summarized in Table 4.5. The R^2s in Table 4.5 were computed following

recommendations in Berthouex and Brown (2002) and represent the amount or variance in the actual temporal trend of ρ_d that is explained by given model simulation. Higher R^2s were obtained via computing ρ_d according to Procedure 2 relative to Procedure 1 for both the Design and Operation assessment, which supports the improved visual fit of these simulations in Fig. 4.11. The most statistically significant ρ_d prediction for the Design assessment was obtained for Procedure 2 and a COT of 70 % (R^2 = 0.93), whereas R^2 = 0.81 for both COTs considered for the Operation assessment. Similar R^2s for the Operation assessment with COT = 70 % and 90 % were anticipated since the actual COT was used during Years 1-4 (Tables 3.5 and 3.6), which was the time period of ρ_d comparison (Fig. 4.11). The negative R^2s corresponding to the Design assessment using Procedure 2 (Table 4.5) are a result of computing a larger sum of squares of residuals relative to total sum of squares; i.e., the mean of the measured data is a better predictor relative to the prediction curve. Therefore, the prediction curve with negative R^2 provides poor predictive performance as shown in Fig. 4.11a.

Procedure 1 yielded lower predicted ρ_d relative to actual ρ_d since Procedure 1 incorporated C_p output from FSConsol that assumes complete saturation of tailings. The actual degree of saturation in a large impoundment varies due to the dynamic deposition strategy along the impoundment perimeter, and unsaturated conditions can enhance consolidation and densification of the impoundment (Wels and Robertson 2003). Barrera and Ortiz (2010) reported moisture retention for different fines contents and tailings from Chilean copper mines, which suggest that tailings do not remain saturated. Similarly, Wels et al. (2004) reported a degree of saturations between 80 % to 90 % for the Pampa de Pabellon tailings impoundment in the upper 0.6 m - 1.0 m of the tailings profile.

The ρ_d technique in Procedure 2 (Fig. 3.13) factored in the actual impoundment volume based on impoundment height prediction and total dry tailings mass discharged to the impoundment to compute ρ_d. Thus, Procedure 2 is more representative of the bulk impoundment

volume, particularly in a large-scale facility that stores millions of cubic meters of tailings and covers hundreds of square meters in surface area.

4.3.2 Impoundment Capacity and Height

Estimates of impoundment capacity (in dry tailings mass) and height were completed based on ρ_d computed from Procedures 1 and 2 (Fig. 3.13). Tailings impoundment height output from FSConsol was used directly in Procedure 2, and thus, all references made to impoundment height estimated via Procedure 2 reflect height predicted directly via FSConsol. The impoundment capacity refers to the maximum storage of overflow (fine product of cycloning) and whole tailings (tailings directly sent from the thickeners), excluding the amount of underflow tailings produced for embankment construction (Fig. 3.9). Total predicted impoundment capacity in dry mass of tailings and total filling time for the Design and Operation assessments are summarized in Table 4.6. Comparisons of annual predicted impoundment capacity in dry mass of tailings for the Design and Operation assessments with COT = 70 % versus actual impoundment capacities for the first 4 yr of operation are shown in Fig. 4.13. The Operation assessment incorporated the actual tailings production rate during Years 1-4 and the future anticipated production rate of 120,000 mtpd, which decreased filling durations compared to the Design assessment as a greater amount of tailings were disposed for similar elapsed times. These operational conditions let to closer comparisons between predicted and actual impoundment capacity during Years 1-4 for the Operation assessment (4.13). The total filling time and impoundment capacity increased as COT increased from 70 % to 90 % in the Operation assessment (Table 4.6) due to less fine tailings (overflow) discharged per day to the TSF.

Differences in impoundment capacity (in volume) and impoundment height between the Operational assessment and actual measurements for the first 6 yr of operation are summarized in Table 4.7. Actual COTs were applied in the Operational assessment for Years 1-4 and a COT = 70 % for all subsequent years (Table 3.5). Impoundment capacity and impoundment height

were overestimated for each year of the comparison when using Procedure 1 to estimate ρ_d, whereas Procedure 2 led to overestimates of impoundment capacity in all years except Year 6 and overestimates of height for all years except Years 5 and 6 (Table 4.7). Differences in capacity range from 5.6 % to 16.9 % and -7.9 % to 9.9 % for Procedure 1 and 2, respectively (Table 4.7). The overestimations of impoundment capacity are consistent with higher actual ρ_d (Fig. 4.11b), which results in a larger mass of tailings retained within a lower total impoundment volume. Differences in surface height of tailings between predictions and actual measurements were lower relative to capacity predictions, ranging from 2.2 % to 6.0 % and -3.0 % to 3.4 % for Procedure 1 and 2, respectively (Table 4.7).

Temporal comparisons of predicted impoundment height using Procedures 1 and 2 to compute ρ_d for the Operation assessment versus actual impoundment height are shown in Fig. 4.14. Trends in predicted surface height for all scenarios considered in the Operation assessment (i.e., Procedures 1 and 2 and COT = 70 % and 90 %) show good agreement with impoundment height measured in the full-scale copper TSF. This close agreement is particularly noteworthy considering operational factors that could affect tailings behavior and impoundment rising that are not taken into consideration in consolidation modeling with FSConsol, such as heterogeneity in tailings characteristics throughout the TSF.

The lower ρ_d estimated with Procedure 1 for the Operation assessment (Fig. 4.11b) implies that more water is retained in the tailings pore space, which increased total tailing volume and leads to an overprediction of impoundment height (Fig. 4.14a). Impoundment height predicted via Procedure 2 (i.e., FSConsol output) also leads to a modest overprediction of impoundment height during the first four years of operation , whereas from Year 5 there is an underprediction (as shown in Fig. 4.14b and described in Table 4.7). The lower ρ_d when compared to actual ρ_d during the first four years causes the slight overestimation described previously; however, from Year 5 onward the underprediction is due to potential overestimation of average ρ_d, as actual ρ_d may

become stable as shown in Fig. 4.11b. For example, comparison between predicted tailings heights and actual tailings heights for the first 6 yr of operation for the Design and Operation assessments with COT of 70 % (shown in Fig. 4.15) exhibited a steady overestimation when Procedure 1 was used, whereas with Procedure 2 there is a transition after year 5.

Vick (1983) reported that tailings ρ_d in full-scale TSFs typically ranges between 1.12 Mg/m^3 (70 pcf) and 1.44 Mg/m^3 (90 pcf) for fine-grained copper tailings with G_s ranging from 2.6 and 2.8. Barrera (1998) reported that average tailings ρ_d ranged between 1.24 Mg/m^3 and 1.38 Mg/m^3 in six copper TSFs with average G_s = 2.7. Similarly, Cacciuttolo (2012) reported that copper tailings G_s = 2.7 had an average ρ_d = 1.30 Mg/m^3 once the large copper Los Quillayes TSF reached full capacity after 10 yr of operation. The reported ρ_ds in Barrera (1998) and Cacciuttolo (2012) agree with the ρ_d range reported in Vick (1983) and suggest that tailings ρ_d in full-scale copper TSFs can be expected to range between approximately 1.12 and 1.44 Mg/m^3.

The average ρ_d in the full-scale copper TSF evaluated in this study reached 1.44 Mg/m^3 after 4 yr of operation. Based on the compilation of copper tailings ρ_d in Vick (1983), Barrera (1998), and Cacciuttolo (2012), only a modest increase in ρ_d may be expected for the remainder of the TSF operation. As a point of comparison, monthly average compacted field ρ_d of underflow tailings (i.e., coarser-grained tailings) used for the embankment dam at the TSF evaluated in this study ranged from 1.63 to 1.69 Mg/m^3 for three consecutive years. Similarly, Lara (2000) reported that the compacted ρ_d of sand embankments at five Chilean TSFs with similar G_s and copper ore mineralogy to this study ranged between 1.60 to 1.70 Mg/m^3. Lower ρ_d for impounded tailings should be expected relative to ρ_d obtained via a compaction test since the level of energy applied in a compaction test is designed to simulate a high energy system, whereas densification of tailings in a TSF replicates a natural sedimentation process with energy applied via tailings self-weight.

The continued increase in ρ_d predicted for either the Design or Operation assessments with Procedure 2 shown in Fig. 4.11 may lead to an overestimation of ρ_d, and an upper-bound ρ_d may need to be applied to truncate predicted ρ_d to represent actual anticipated field conditions. However, observations and comparisons of tailings ρ_d in full-scale TSFs are only anecdotal and the field data evaluated in this study are not sufficient to confirm a potential upper-bound of ρ_d. An overestimation in ρ_d will lead to a longer estimated filling time and final impoundment capacity, which can be viewed as unconservative from the perspective of a mine owner or engineer. The modeling procedure in FSconsol considers progressive consolidation from the deepest portion of the discretized impoundment, which may lead to higher tailings ρ_d when compared to field average ρ_d values that cover variable depths within the impoundment.

4.3.3 Practical Implications

The consistency of the predicted ρ_d with Procedure 2 for the Design and Operation assessments versus field average ρ_d suggests that the design conditions for the full-scale TSF were adequate to satisfactorily design the TSF. However, ρ_d estimated with Procedure 2 for the Design assessment yielded the highest ρ_d predictions (Fig. 4.11), which may lead to an overestimation of impoundment capacity and service life of the TSF. Tailings ρ_d estimated with Procedure 2 for the Operation assessment yielded a good overall fit to actual ρ_d and lower long-term ρ_d predictions. These observations support the periodic re-evaluation of tailings consolidation modeling during operation to reflect actual conditions and update impoundment capacity and projected lifespan for appropriate future planning.

The ρ_d calculation in Procedure 2 yielded more comparable results relative to the field average ρ_d versus the ρ_d calculation in Procedure 1, which underestimated the field average ρ_d. These comparisons of ρ_d support the use of Procedure 2 to estimate ρ_d and associated

operational parameters (e.g., impoundment capacity, filling time) for full-scale TSFs. However, a maximum ρ_d should be considered when using the ρ_d estimation technique outlined in Procedure 2. The assessment of a maximum tailings ρ_d can be based on observations reported herein, but should also reflect an engineer's experience on the design of other tailings impoundments with similar characteristics. Good practice would be to conduct a sensitivity analyses of COT, underflow recovery, and maximum ρ_d values during final engineering design to assess a potential range in anticipated impoundment capacity and filling time to guide decision making.

Impoundment heights used in the ρ_d calculation approach in Procedure 2 were direct output from FSConsol outputs and appear to be an appropriate representation of tailings consolidation behavior in a full-scale TSF, particularly during the first few years of operation. The good comparison between impoundment height predicted with FSconsol can instill confidence in the mine owner or engineer to apply 1-D model simulations of consolidation behavior to full-scale planning of a TSF.

Table 4.1. Summary of one-dimensional large-strain consolidation results instantaneous tailings deposition benchmark example from Townsend and McVay (1990) as well as simulation results from modeling conducted in CONDES0 and FSConsol.

Model simulation	Final tailings height	Results at end of Year 1	
		Tailings height	Void ratio at base of column
	(m)	(m)	
Average of predictions [a]	4.16 (0.05)[b]	7.19 (0.42)	6.58 (0.22)
CONDES0	4.18	6.73	6.53
FSConsol	4.13	6.81	6.42

[a] Nine modeling teams provided 12 predictions for settlement and 10 predictions for void ratio (Townsend and McVay 1990)

[b] Standard deviation in parentheses

Table 4.2. Summary of total filling time and impoundment capacity for the continuous tailings deposition benchmark example in Gjerapic et al. (2008) as well as model simulation results from FSConsol and CONDES0.

Model simulation	Total filling time (yr)	Total tailings capacity based on dry mass (Mg)
Gjerapic (upper solution)	14.60	10.6×10^6
FSConsol (13.33 m)	11.37	8.3×10^6
FSConsol (4 m)	13.26	9.7×10^6
FSConsol (1 m)	14.11	10.3×10^6
CONDES0 (13.33 m)	10.11	7.4×10^6

Table 4.3. Impoundment capacity, predicted total filling time, and average dry densities for five different tailings impoundment side-slope configurations simulated in FSConsol. Truncated square pyramid with 100-m-wide base and 10-m-tall side slopes used for as the impoundment facility.

Side slope	Total volume of truncated square pyramid [a] (m^3)	Total filling time (yr)	Total tailings capacity based on dry mass (Mg)	Average dry density (Mg/m^3)	
				At full capacity [b]	After 4 yr of simulation [c]
1.0H:1V	121,333	5.2	191,000	1.574	1.550
2.0H:1V	145,333	6.3	229,000	1.576	1.538
2.5H:1V	158,333	6.8	250,000	1.579	1.532
3.5H:1V	186,333	8.1	294,000	1.578	1.522
4.5H:1V	217,000	9.4	343,000	1.581	1.513

[a] Available volume capacity based on impoundment geometry.

[b] Average dry density when filling is complete.

[c] Average dry density after 4 yr of simulation time.

Table 4.4. Predicted filling times and impoundment capacities based on FSConsol results for various production rates and side-slope configurations within a theoretical tailings basin modeled as a truncated square pyramid with 100-m-wide base and 10-m-tall side slopes.

	4.5H:1V		3.5H:1V		2.5H:1V		2.0H:1V		1.0H:1V	
Tailings production rate (mtpd)	Total filing time (yr)	Basin Capacity (Mg)	Total filling time (yr)	Basin Capacity (Mg)	Total filling time (yr)	Basin Capacity (Mg)	Total filling time (yr)	Basin Capacity (Mg)	Total filling time (yr)	Basin Capacity (Mg)
50	18.8	343,500	16.2	295,000	13.8	251,000	12.6	230,000	10.5	192,000
100	9.4	343,000	8.1	294,000	6.8	250,000	6.3	229,000	5.2	191,000
200	4.7	342,000	4.0	292,000	3.4	248,000	3.1	226,000	2.6	188,000
300	3.1	339,000	2.7	291,000	2.2	246,000	2.1	225,000	1.7	186,000

Table 4.5. Summary of range in tailings dry density (ρ_d) and coefficient of determination for Design and Operation assessments of the full-scale copper tailings storage facility evaluate with with Procedures 1 and 2 for cyclone operation times (COTs) of 70 % and 90 %.

Assessment	ρ_d calculation procedure	COT %	Range of ρ_d for Years 1 - 4 [a] Mg/m^3	R^2
Design	Procedure 1	70	1.004 - 1.234	-0.48
		90	0.914 - 1.149	-2.30
	Procedure 2	70	1.046 - 1.473	0.93
		90	0.958 - 1.397	0.42
Operation	Procedure 1	70	1.086 - 1.255 [b]	0.09
		90		
	Procedure 2	70	1.132 - 1.374 [b]	0.81
		90		

Note: COT = percentage of time that the cyclone station is in operation; R^2 = coefficient of determination.

[a] Range of actual average ρ_d collected during the first 4 yr of operation of the full-scale TSF = 0.997 - 1.436 Mg/m^3.

[b] Predicted ρ_d values are the same for either COT values since same actual data were used for modeling during the first 6 yr.

Table 4.6. Predicted total filling times and impoundment capacities for model simulations in the Design and Operation assessments with Procedures 1 and 2 completed for the full-scale tailings storage facility case study.

Assessment and cyclone operation time (COT)	Procedure 1		Procedure 2	
	Time (yr)	Final capacity in dry tailings mass (Mg)	Time (yr)	Final capacity in dry tailings mass (Mg)
Design, COT = 70 %	27.3	814.3×10^6	31.6	942.6×10^6
Design, COT = 90 %	28.6	776.3×10^6	33.4	907.9×10^6
Operation, COT = 70 %	24.0	774.5×10^6	26.6	863.5×10^6
Operation, COT = 90 %	26.3	784.9×10^6	29.8	893.0×10^6

Table 4.7. Predicted annual total volumetric capacity (in millions, M, of cubic meters) and impoundment height of the full-scale tailings storage facility for the Operation assessment with 70 % cyclone operation time assumed for Years 5 and 6. Actual annual volumetric capacity and impoundment height listed as "field data" along with percent differences between model simulations and field data.

Model Simulation Year	Procedure 1		Procedure 2		Field data		Field data compared to Procedure 1		Field data compared to Procedure 2	
	Annual total capacity (Mm^3)	Impound-ment height (m)	Annual total capacity (Mm^3)	Impound-ment height [a] (m)	Annual total capacity (Mm^3)	Impound-ment height [b] (m)	Capacity difference (%)	Height difference (%)	Capacity difference (%)	Height difference (%)
1	20.2	68.4	19.4	67.4	18.3	66.7	10.6%	2.6%	6.0%	1.0%
2	42.3	91.6	39.3	89.1	37.3	88.3	13.3%	3.8%	5.4%	0.9%
3	65.0	108.8	60.8	106.1	55.3	102.6	17.5%	6.0%	9.9%	3.4%
4	86.2	121.6	78.8	117.4	73.8	116.9	16.9%	4.0%	6.8%	0.5%
5	109.2	133.1	97.5	127.5	94.9	128.4	15.1%	3.6%	2.7%	-0.7%
6	130.6	142.6	114.0	135.4	123.7	139.6	5.6%	2.2%	-7.9%	-3.0%

[a] Predicted heights directly taken from FSConsol (height output).

[b] Average impoundment height measured at crest of the full-scale tailings storage facility.

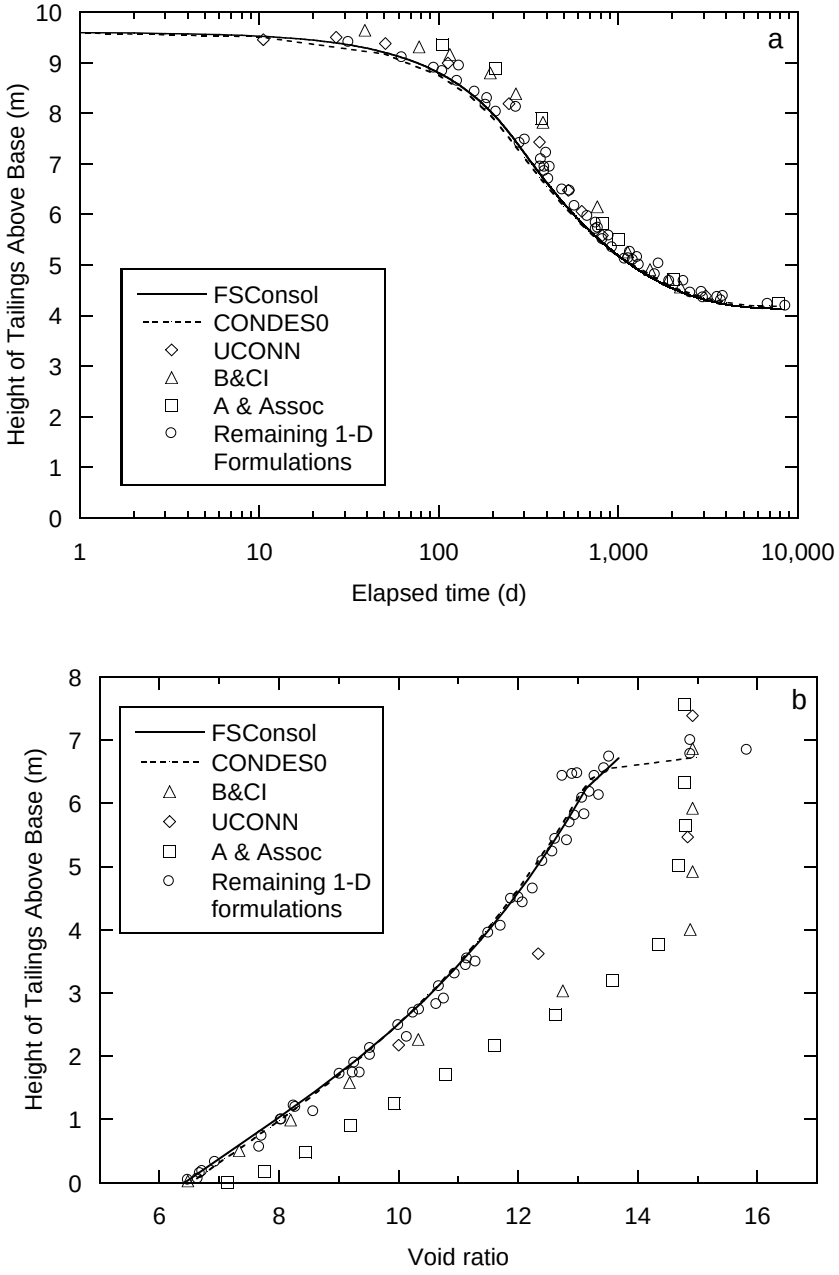

Fig. 4.1. One-dimensional consolidation modeling results for the instantaneous benchmark example in Townsend and McVay (1990): (a) temporal trends of height of tailings from twelve predictions in Townsend and McVay (1990), CONDES0, and FSconsol; and (b) void ratio profiles the end of Year 1 for ten predictions in Townsend and McVay (1990), CONDES0, and FSConsol.

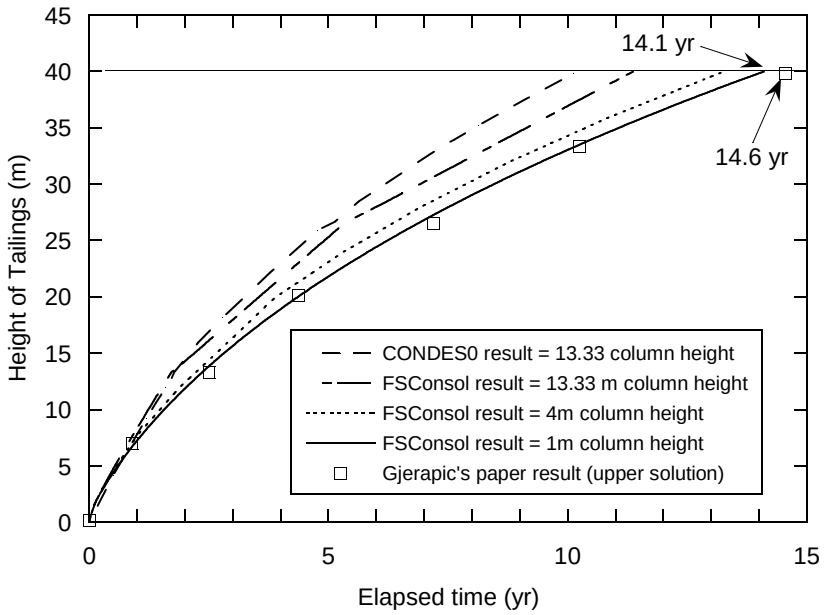

Fig. 4.2. Temporal relationships of tailings height for the continuous tailings deposition benchmark example in Gjerapic et al. (2008). Model simulations shown for FSConsol considering impoundment discretized into 1-m-, 4-m-, and 13.33-m-tall columns; CONDES0 results only based on impoundment discretization into three 13.33-m-tall columns. Continuous deposition was stopped once height of tailings = 40 m; thus, stop time in simulation = filling time.

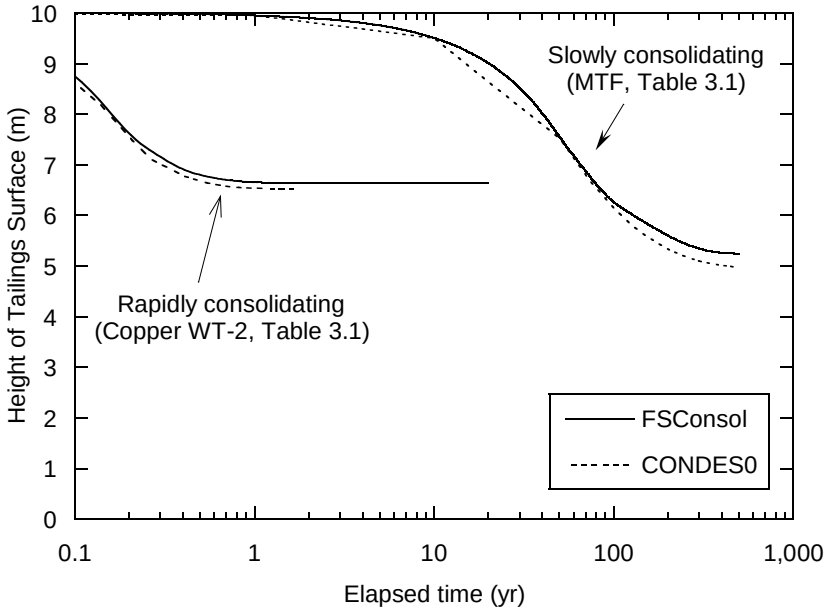

Fig. 4.3. Temporal trends of tailings surface height (i.e., settlement) for model simulations conducted in CONDES0 and FSConsol for an instantaneously filled column considering slowly consolidating tailings (SCT) with k = 1.10 x $10^{-11} \cdot e^{3.79}$ (m/s) and rapidly consolidating tailings (RCT) with k = 1.02 x $10^{-7} \cdot e^{3.42}$ (m/s). Note: k = hydraulic conductivity and e = void ratio.

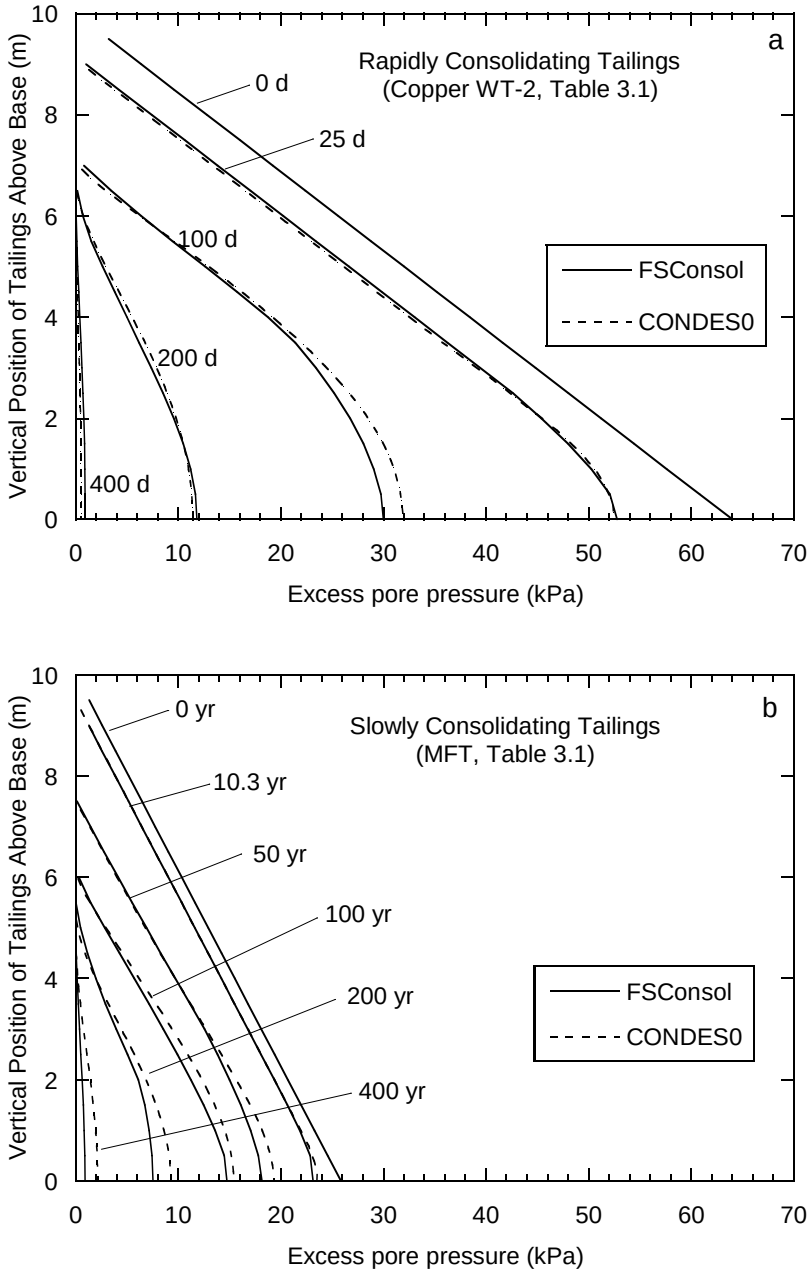

Fig. 4.4. Profiles of excess pore water pressure (u_e) at different elapsed times based on model simulations in CONDES0 and FSConsol of an instantaneously filled column considering (a) rapidly consolidating tailings (RCT) and (b) slowly consolidating tailings (SCT).

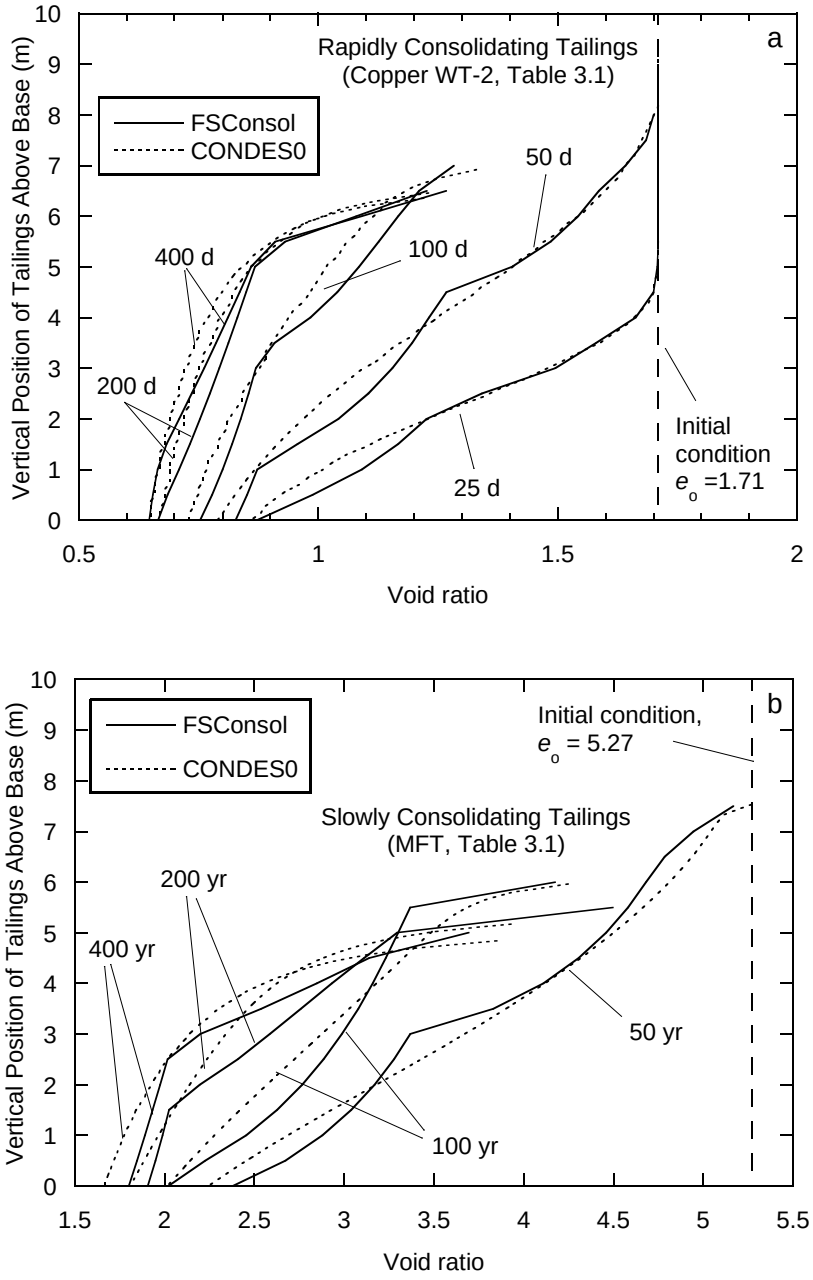

Fig. 4.5. Profiles of void ratio at different elapsed times based on model simulations in CONDES0 and FSConsol of an instantaneously filled column considering (a) rapidly consolidating tailings (e = 1.30 $(\sigma'+0.192)^{-0.168}$) and (b) slowly consolidating tailings (e = 3.52 $(\sigma'+0.181)^{-0.236}$).

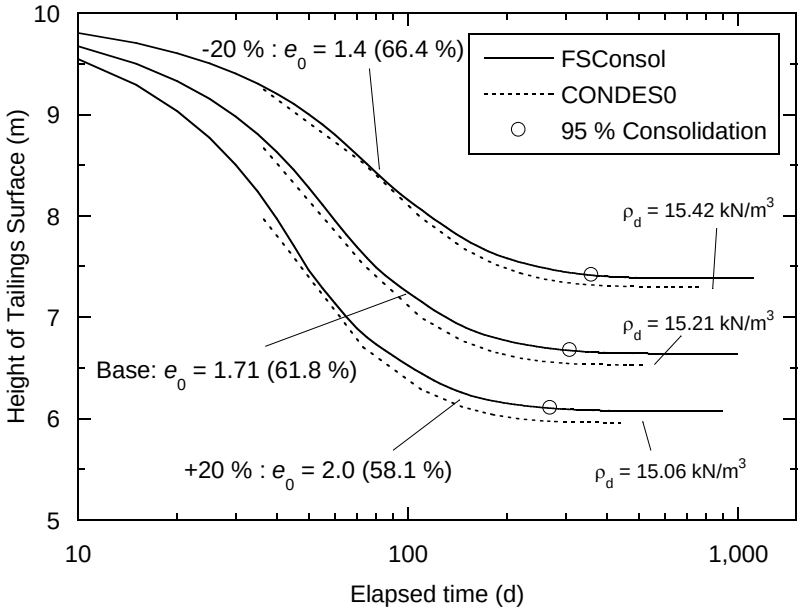

Fig. 4.6. Temporal trends of tailings surface height based on model simulations in FSConsol and CONDES0 of an instantaneously filled column considering different initial void ratio (e_o) for copper whole tailings (WT-2). Circle on curve represents time at which 95% consolidation is achieved; average dry densities (ρ_d) listed for complete consolidation.

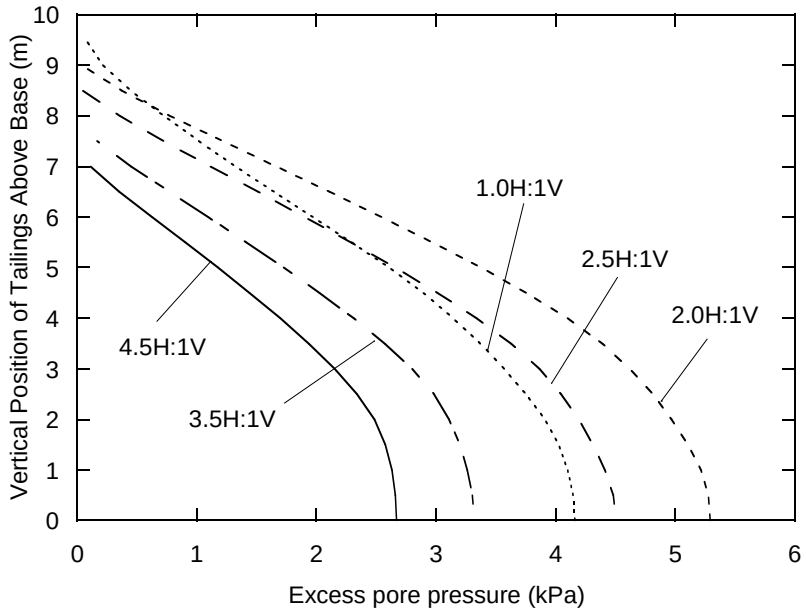

Fig. 4.7. Profiles of excess pore pressure at an elapsed time of 5.5 yr (2000 d) based on model simulations in FSConsol for gradual tailings deposition into an inverted square frustum with a 100-m-wide base, 10-m-tall sides slopes, and different horizontal (H) to vertical (V) side-slope configurations.

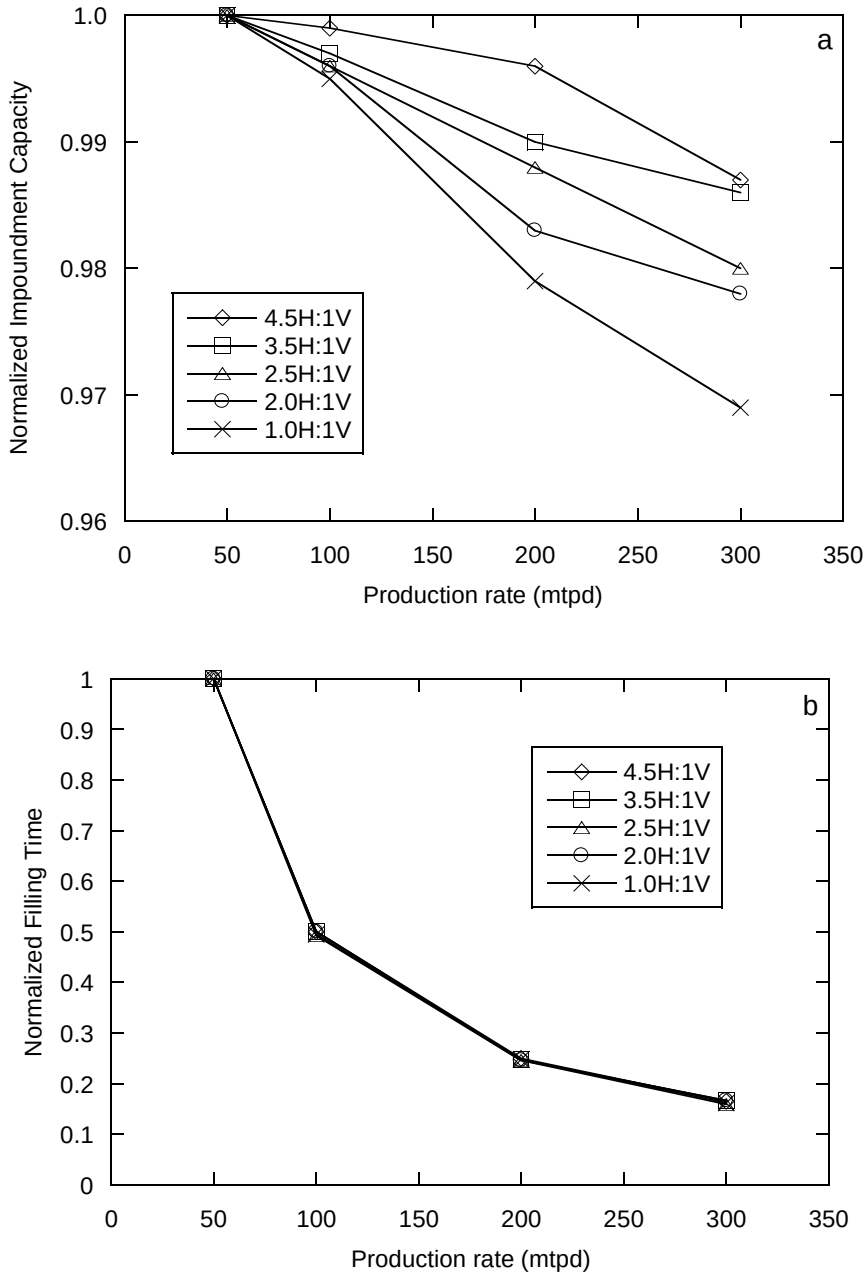

Fig. 4.8. Relationships of normalized impoundment capacity and normalized filling time as a function of tailings production rate based on model simulations in FSConsol for graduate tailings deposition into an inverted square frustum with a 100-m-wide base, 10-m-tall sides slopes, and different horizontal (H) to vertical (V) side-slope configurations. Capacity and filling time normalized to results for a tailings production rate of 50 mtpd.

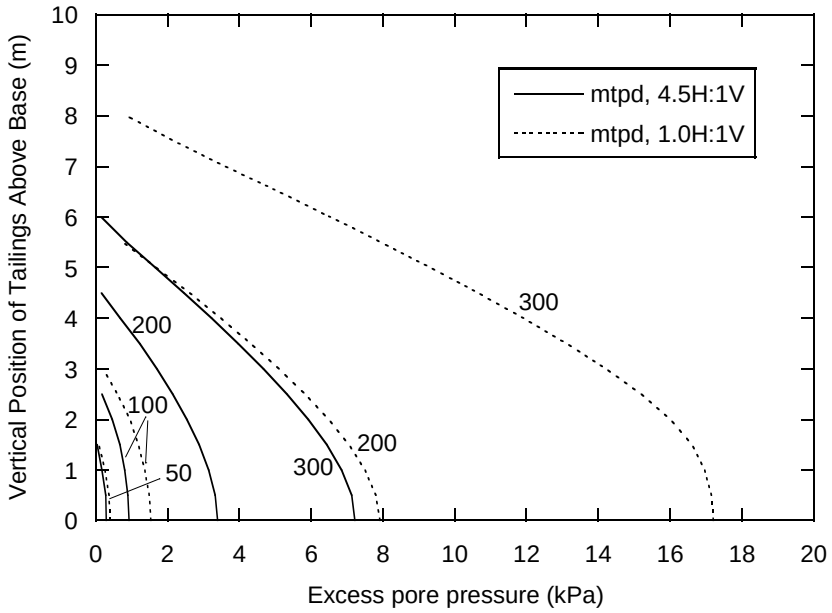

Fig. 4.9. Profiles of excess pore pressure at an elapsed time of 1.4 yr (500 d) based on model simulations in FSConsol for gradual tailings deposition into an inverted square frustum with a 100-m-wide base, 10-m-tall sides slopes, and horizontal (H) to vertical (V) side-slope configurations of 1.0H:1.0V and 4.5H:1.0V. Results presented for tailings production rates ranging from 50 to 300 mtpd.

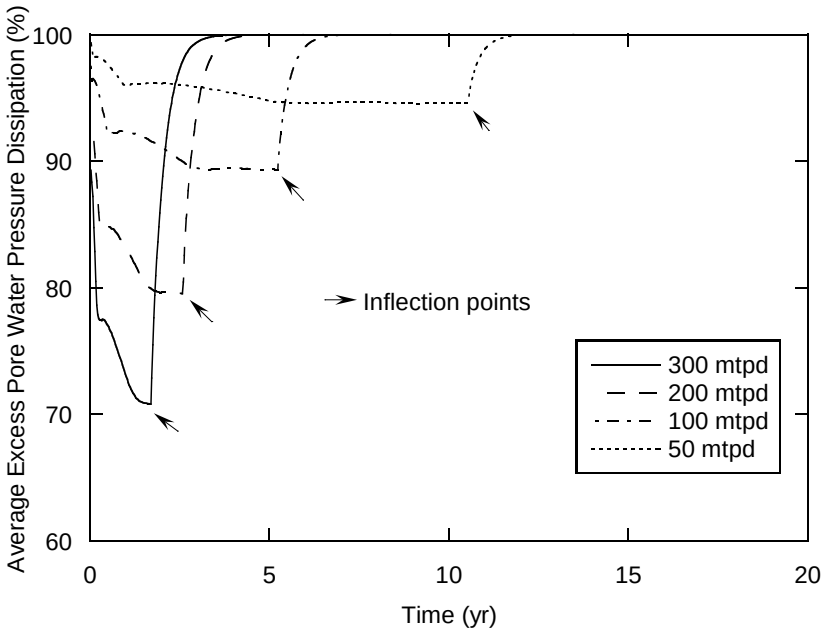

Fig. 4.10. Temporal relationships of average excess pore water pressure dissipation based on model simulations in FSConsol for gradual tailings deposition into an inverted square frustum with a 100-m-wide base, 10-m-tall sides slopes, and horizontal (H) to vertical (V) side-slope configuration of 1.0H:1.0V. Results presented for tailings production rates ranging from 50 to 300 mtpd and the inflection point represents time to reach complete filling of the impoundment.

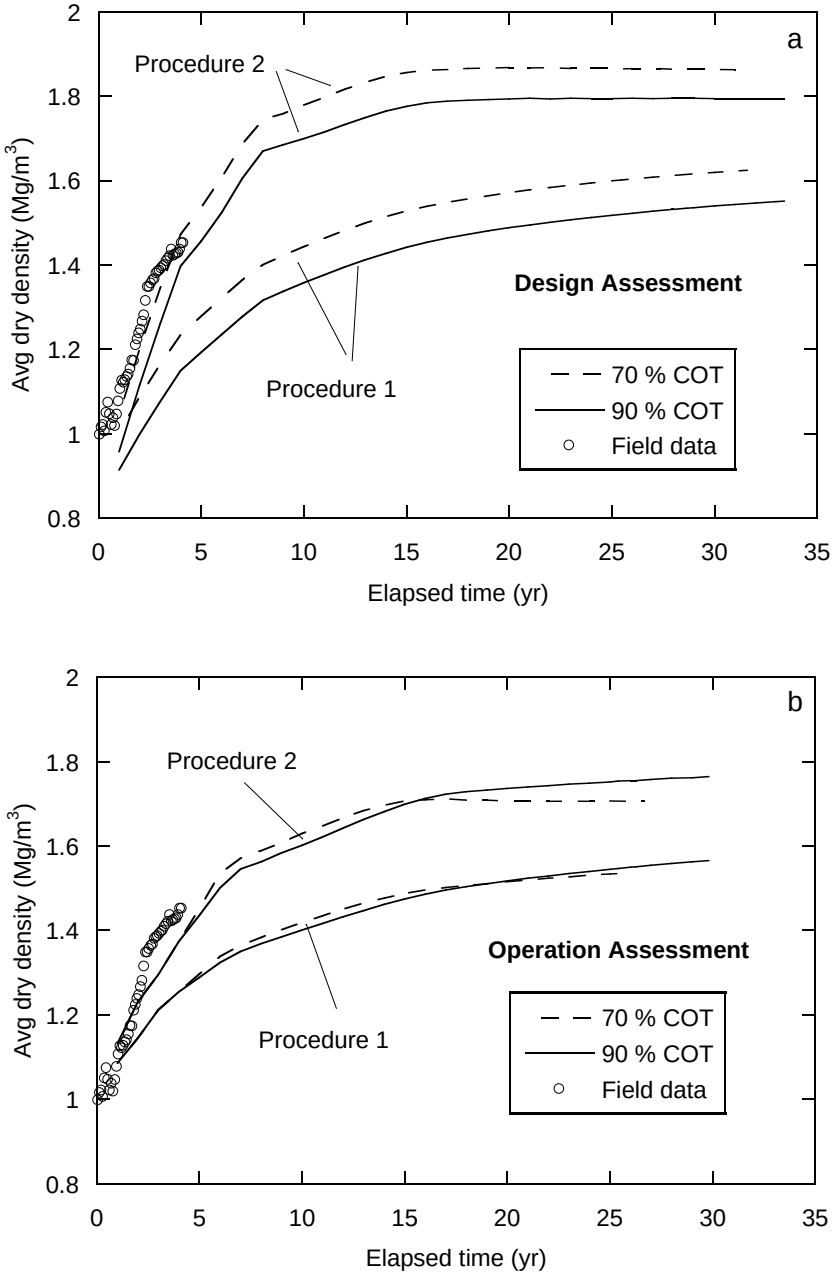

Fig. 4.11. Temporal relationships of actual and predicted average dry tailings density in the full-scale tailings storage facility. Model simulation results presented for the (a) Design and (b) Operation assessment considering dry density calculations in Procedure 1 and 2. Procedure 1 used solids content predicted by FSConsol and Procedure 2 used impoundment height and dry tailings mass discharged into the impoundment predicted by FSConsol with the actual height-to-volume relationship for the tailings storage facility (Fig. 3.13).

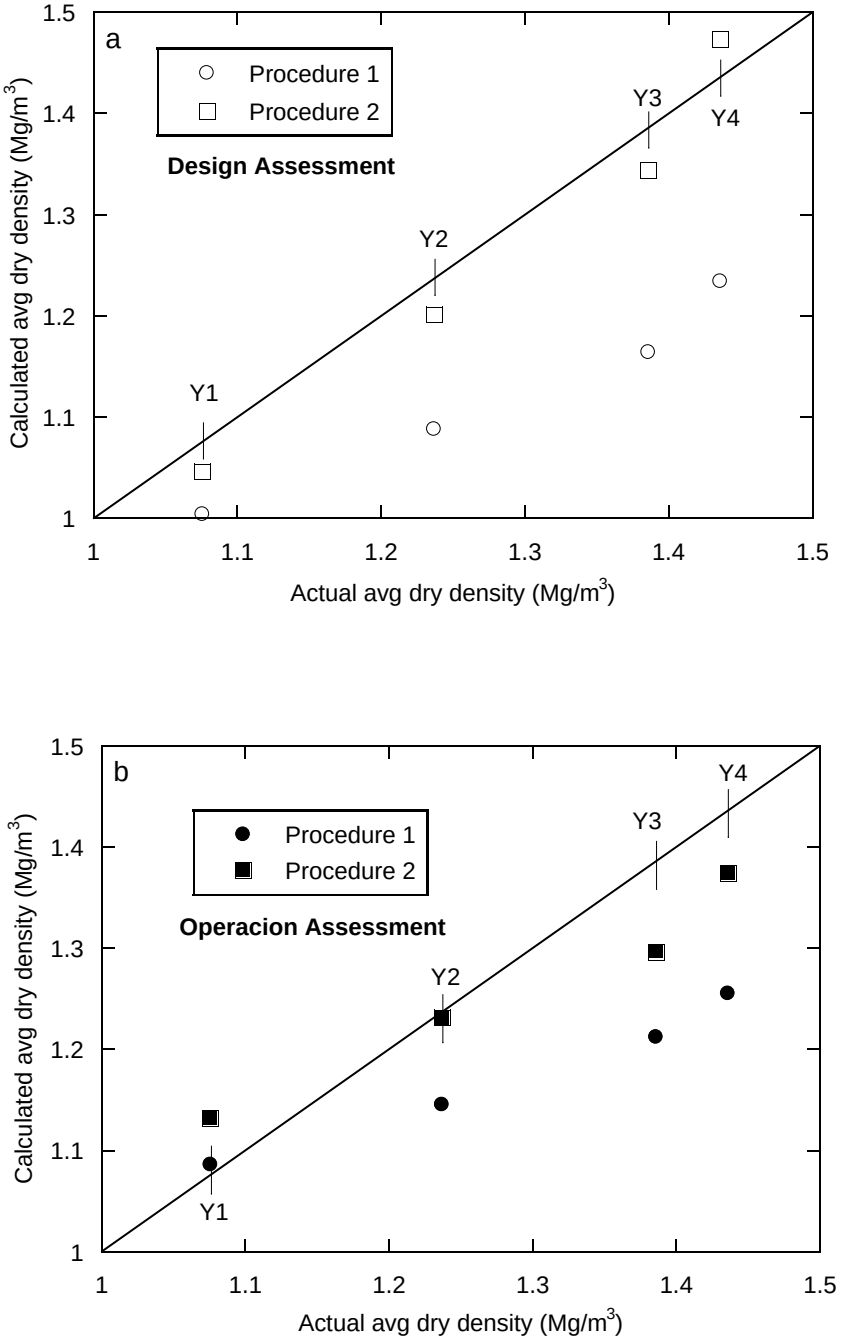

Fig. 4.12. Comparison of predicted average dry tailings density to actual tailings dry density in the full-scale tailings storage facility. Model simulation results representative of the first four years shown for the (a) Design assessment and (b) Operation assessment with a cyclone operation time (COT) of 70 % considering dry density calculation Procedures 1 and 2 (Fig. 3.13). Yi = Year i (i=1, 2, 3, 4)

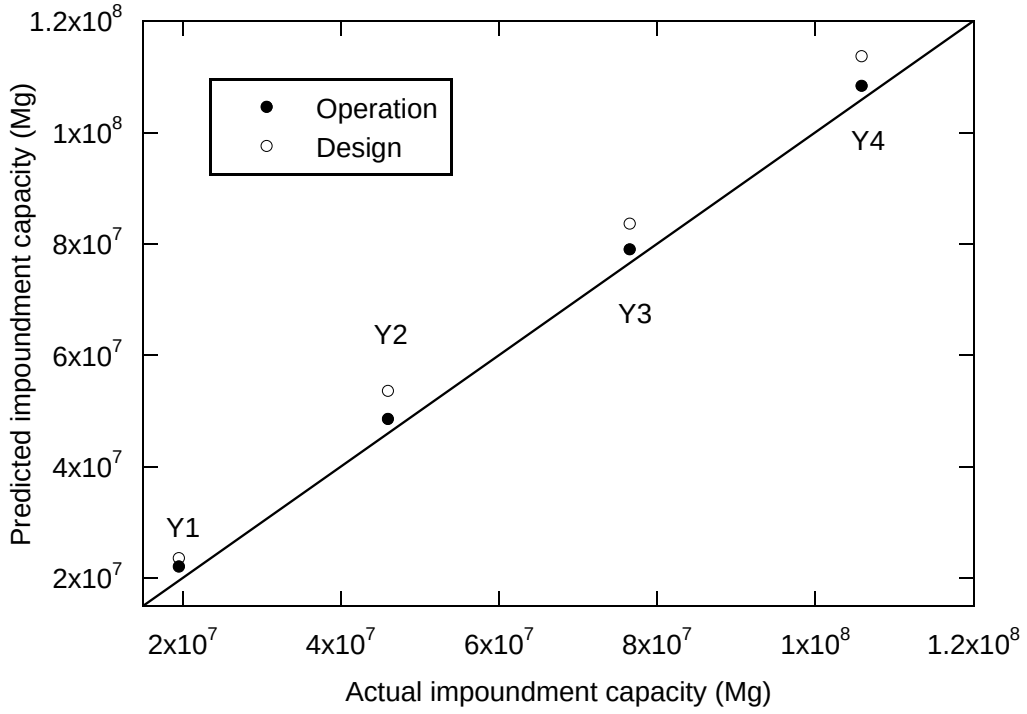

Fig. 4.13. Comparison of predicted impoundment capacity to actual impoundment capacity of the full-scale tailings storage facility. Model simulation results representative of the first four years shown for the (a) Design assessment and (b) Operation assessment with a cyclone operation time (COT) of 70 %. Yi = Year i (i=1, 2, 3, 4)

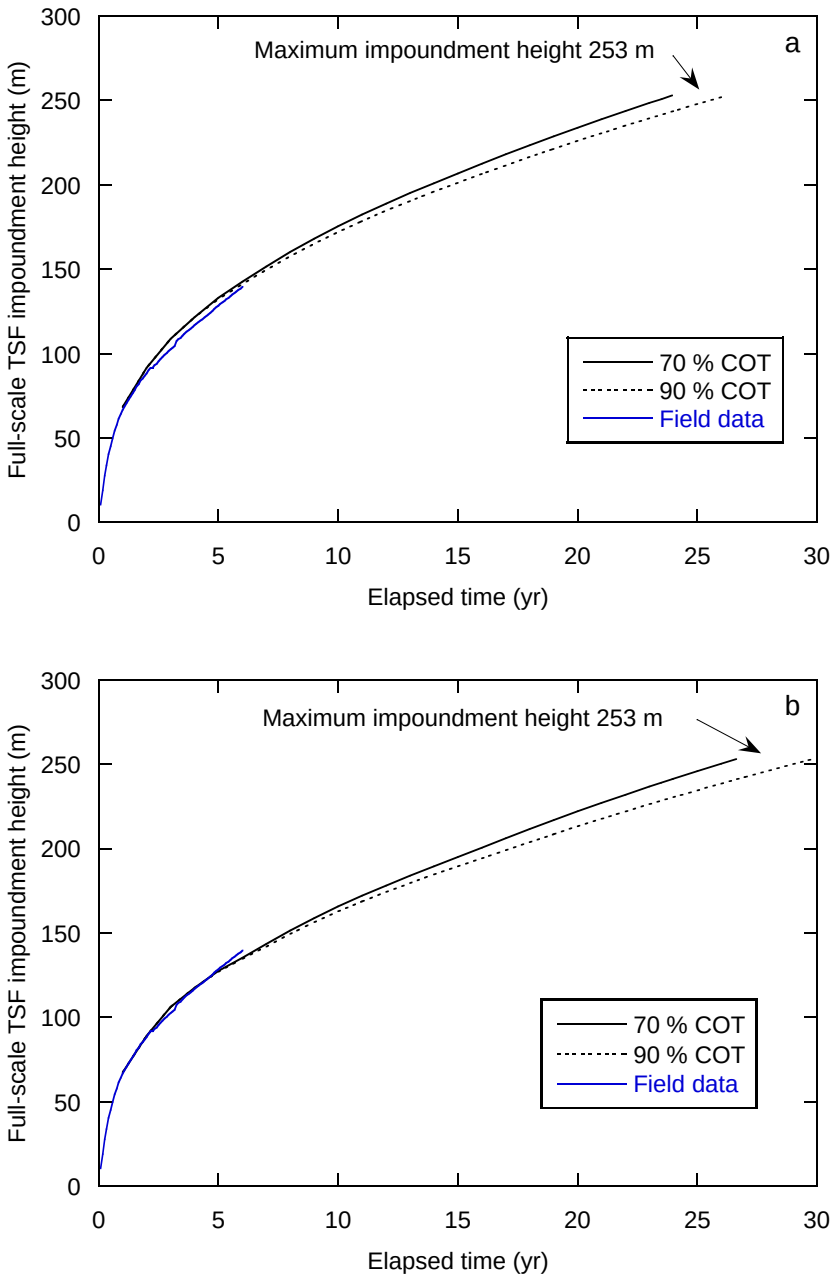

Fig. 4.14. Temporal relationships of actual and predicted impoundment height in the full-scale tailings storage facility. Model simulation results presented for the Operation assessment considering dry density calculations in (a) Procedure 1 and (b) Procedure 2 and a cyclone operation time of 70 and 90% from Year 5 until the end of the model simulation. Procedure 1 used solids content predicted by FSConsol and Procedure 2 used impoundment height and dry tailings mass discharged into the impoundment predicted by FSConsol with the actual height-to-volume relationship for the tailings storage facility (Fig. 3.13).

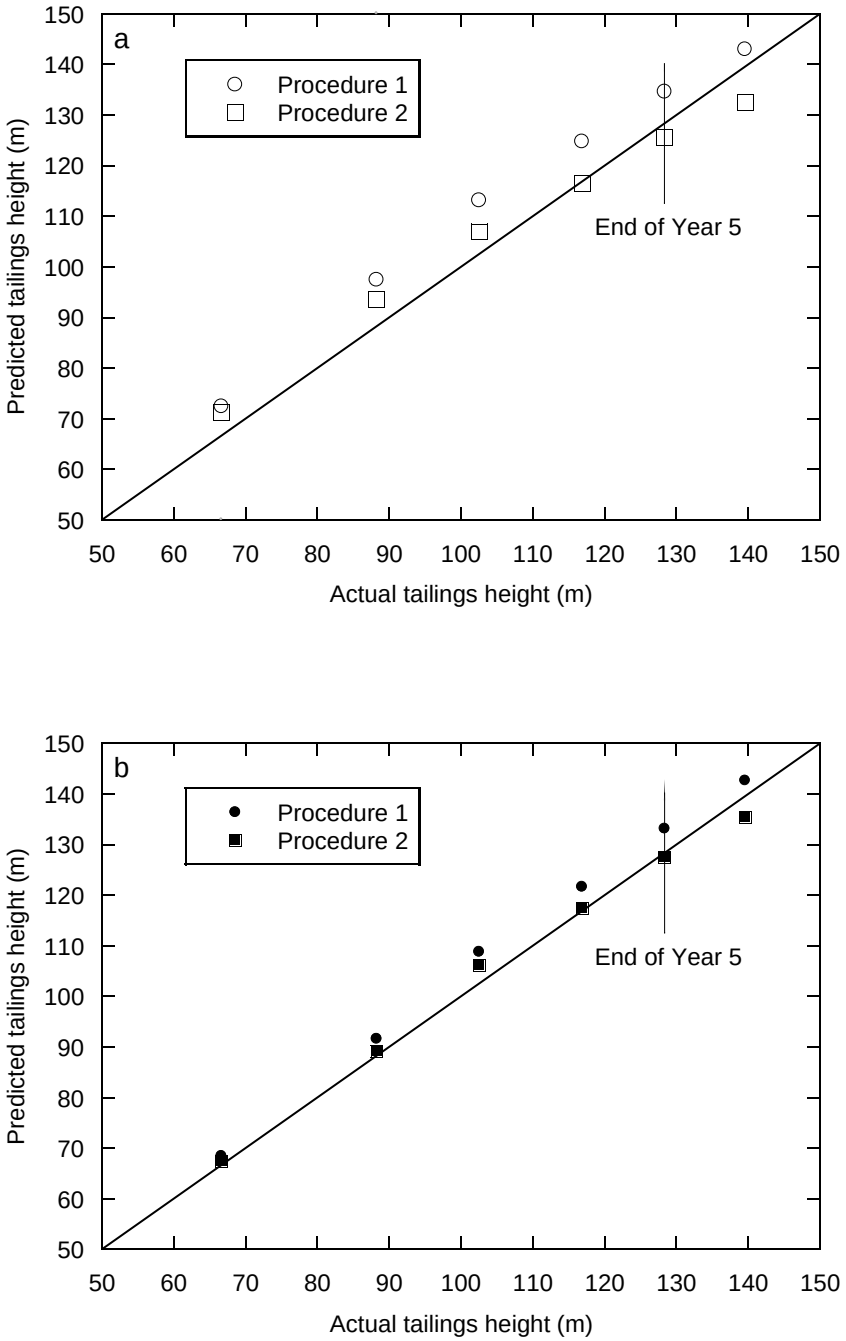

Fig. 4.15. Comparison of predicted tailings height to actual tailings height of the full-scale tailings storage facility. Model simulation results representative of the first six years shown for the (a) Design assessment and (b) Operation assessment with a cyclone operation time (COT) of 70 % and Procedure 1 and 2.

CHAPTER 5: SUMMARY, CONCLUSIONS, AND FUTURE WORK

5.1 Summary and Conclusions

The applicability of two commercially-available, one-dimensional (1-D), large-strain consolidation programs (FSConsol and CONDES0) in predicting the consolidation behavior of mine tailings was evaluated via benchmark examples from literature, a parametric study, and a full-scale tailings storage facility (TSF) case study. Two benchmark examples were selected to represent instantaneous and gradual deposition of tailings. The parametric study was conducted to examine the influence of input parameters on consolidation behavior. Finally, the case study was used to evaluate the efficacy of applying a 1-D model to predict dry density, impoundment capacity, and surface height of a full-scale TSF for a large copper mine. Design and Operation assessments were considered in the full-scale TSF analysis to include design criteria parameters (Design) and actual average parameters measured during TSF operation (Operation). Model results were compared to operational data, which included 4 yr of average tailings dry density and 6 yr of tailings height within the impoundment.

FSConsol and CONDES0 yielded similar consolidation behavior in the benchmark example of instantaneous tailings deposition, and both compared favorably to results from literature. For example, the final height from the simulation conducted in CONDES0 and FSConsol was 4.18 m and 4.13 m, respectively, compared to the average final height of 4.16 m from literature (Townsend and McVay 1990). FSConsol was found to be more applicable relative to CONDES0 in simulating a scenario of gradual tailings deposition based on favorable comparisons to published results and practicality of simulating multiple materials and deposition rates.

The parametric study revealed that tailings constitutive relationships (e-σ', k-e) and initial void ratio (e_0) had more pronounced influence on tailings consolidation behavior relative to

impoundment geometry and production rate. For example, the non-linear hydraulic conductivity-void ratio (*k*-*e*) relationship can increase consolidation time more than 200 yr when hydraulic conductivity was reduced four-orders of magnitude. This prolonged consolidation time can result in the demand of larger TSFs to accommodate daily tailings disposal requirements. Altering the initial void ratio influenced the magnitude of total consolidation settlement and final tailings dry density. For example, a decrease in e_o by 20 % produced an increase in the average final height of 11 % (less settlement) . There is relatively minor variation in ρ_d as a function of side slope (1H:1V to 4.5H:1V). Changes in tailings production rate had limited effect on the impoundment capacity for the range of production rates (50 to 300 mtpd) evaluated in this study. The impoundment dry capacity decreased only 1.3 % and 3.1 % as production rates increased from 50 mtpd to 300 mtpd for 4.5H:1V and 1.0H:1V side slopes, respectively.

Two procedures (Procedure 1 and 2) to calculate average dry density were evaluated in this study. Average dry density of tailings within the TSF was accurately predicted via Procedure 2, which was based on FSConsol predictions of tailings surface height and cumulative dry tailings mass discharged to the impoundment coupled with a surface height-to-volume relationship of the actual impoundment. Tailings dry density predictions incorporating Procedure 2 yielded coefficients of determination of 0.93 for the Design assessment with a cyclone operation time of 70% and 0.81 for the Operation assessment. Procedure 1, which predicted average tailings dry densify based on FSConsol predictions of average tailings solids content, underpredicted actual tailings dry density in all cases. With Procedure 2, good agreement was observed between predicted and actual tailings dry density and tailing height (i.e., impoundment surface) within the full-scale TSF, which indicates that FSConsol is applicable for predicting consolidation behavior in a full-scale TSF. Tailings height within the impoundment presented height differences in the range of 0.5 % to 3.4 % when compared to actual heights for the first six years of operation of the large-scale TSF.

Based on satisfactory results of modeling the full-scale TSF case, 1-D consolidation modeling is applicable to predict the tailings consolidation behavior at full-scale. FSConsol uses surface area and filling rate to determine filling flux in order to represent the deposit as a 1-D column in the middle of the deposit.

5.2 Future Work

The present research considered only 1-D consolidation analyses to account for three dimensionality of a full-scale TSF during gradual tailings deposition. Also, periodic tailings deposition was assumed evenly distributed over the entire surface of the TSF and that tailings were homogeneous. Further research should be conducted to evaluate full-scale consolidation behavior of tailings considering other computer programs that provide solutions for multi-dimensional large-strain consolidation (i.e., 2-D and 3-D solutions). Additionally, tailings discharged into a full-scale TSF typically exhibit segregation, which can lead to spatial variability in settlement magnitude and rate. Spatial variability of consolidation behavior should be evaluated and compared with observation and actual data from full-scale TSFs.

The dry density of tailings in full-scale copper mine TSFs has been reported to range between approximately 1.12 and 1.44 Mg/m^3 (Vick 1982; Barrera 1998; Cacciuttolo 2012). Model simulations completed for this study with dry density computed via Procedure 2 yielded dry density > 1.7 Mg/m^3 for long-term predictions (i.e., > 20 yr). The practicality of truncating predicted dry density based on empirical data needs to be evaluated. Coupling FSConsol simulation results of consolidation behavior with an upper-bound average tailings dry density has the potential to improve long-term predictions of storage capacity within a full-scale TSF.

REFERENCES

Aubertin M., Bussiere B., and Chapuis R. (1996). Hydraulic conductivity of homogenized tailings from hard rock mines, *Canadian Geotech Journal*, 33: 470-482.

Abu-Hejleh, A. N., and Znidarcic D. (1992). User manual for computer program SICTA, Report prepared for FIPR, Dept, of Civil Engineering, University of Colorado, Boulder, Co.

Abu-Hejleh, A. N., Znidarcic D., and Barnes B. (1996). Consolidation characteristics of phosphatic clays. *Journal of Geotechnical Engineering*, 122(4), pp. 295-301.

Barrera, S. (1998). Deposition densities of tailings in Chilean deposits, Proceedings Tailings and Mine Waste 1998, Colorado State University, Fort Collins, Colorado, pp. 109-116.

Barrera, S., and Ortiz J. (2010). Water retained in tailings: How to reduce it?. *Water in Mining, II International Congress on Water Management in the Mining Industry*, Santiago, Chile.

Berthouex, P. and Brown, L. (2002). Statistics for Environmental Engineers, 2nd Ed., *Lewis Publishers*, Boca Raton, FL.

BGC Engineering Inc. (2010). Oil sands tailings technology review, *Oil Sands Research and Information Network*.

Blight, G.E. (2003). Quantified comparisons of disposal of thickened and unthickened tailings, *Proceedings Tailings and Mine Waste 2003*, Colorado State University, Fort Collins, Colorado, USA, A.A. Balkema Publishers, pp. 63-72.

Bussiere, B. (2007). Colloquium 2004: Hydrogeotechnical properties of hard rock tailings from metal mines and emerging geoenvironmental disposal approaches, *Canadian Geotechnical Journal,* 44: 1019-1052.

Cacciuttolo, C., and Barrera S. (2012). Variation of tailings density in depth: A model, *Proceedings Tailings and Mine Waste 2012*, Colorado State University, Fort Collins, Colorado, pp. 151-162.

Caldwell, J.A., Fergunson K., Schiffman R.L., and Van Zyl D. (1984). Application of finite strain consolidation theory for engineering design and environmental planning of mine tailings impoundments, *Sedimentation Consolidation Models – Predictions and Validation*, 581-606.

Carrier, D., Bromwell L., and Somogyi F. (1983). Design capacity of slurried mineral waste ponds, *Journal of Geotechnical Engineering*, 109(5): 699-716.

Chambers B., Howard P., Pottie J., Murray L., and Burgess A. (2003). Water recovery from a mine in the Atacama desert, *Water in Mining 2003*, Brisbane, Australia.

Coffin, J.G. (2010). *A three-dimensional model for slurry storage facilities*, Ph.D. Dissertation, Department of Civil Engineering, University of Colorado, Boulder, Colorado.

Consoli, N., and Sills, G. (2000). Soil formation from tailings: comparison of predictions and field measurements, *Geotechnique*, 50(1), 25-33.

Da Silva, F. and Graham, M. (2014). Geotextile bags for enhanced dewatering and accelerated consolidation of oil sands mature fine tailings, *Tailings and Mine Waste 2014*, Colorado State University, Fort Collins, Colorado, pp. 425-436.

Dimitrova, R. (2011). Geotechnique, physic-chemical behavior and a new erosion model for mine tailings under environmental loading, Ph.D. Dissertation, Graduate Program in Civil and Environmental Engineering, The University of Western Ontario, Ontario, Canada.

Estepho, M. (2014). Seepage induced consolidation test: characterization of mature fine tailings, M.S. Thesis, The Faculty of Graduate Studies, Mining Engineering, The University of British Columbia, Vancouver.

Fox, P. J. and Berles, J. D. (1997). CS2: a piecewise-linear model for large-strain consolidation, *International Journal for Numerical and Analytical Methods in Geomechanics*, 21(7), 453-475.

Fredlund, M.D., and Gitirana G. (2009). Large-strain 1D, 2D, and 3D consolidation modeling of mine tailings, *SoilVision Systems Ltd, Saskatoon, SK, Canada.*

Geier, D., Gjerapic G., and Morrison K. (2011). Determination of consolidation properties, selection of computational methods, and estimation of potential error in mine tailings settlement calculations, *Proceedings Tailings and Mine Waste 2011*, Norman B. Keevil Institute of Mining Engineering, Vancouver, BC, Canada, pp. 279-291.

Gibson, R.E., England, G.L., and Hussey M.J. (1967). The theory of one-dimensional consolidation of saturated clays, *Geotechnique*, 17(3), 261-273

Gjerapic, G., Johnson J., Coffin J., and Znidarcic D. (2008). Determination of tailings impoundment capacity via finite-strain consolidation models, *GeoCongress 2008*, ASCE, pp. 798-805.

Henderson, M. (1999). Control and optimization of tailings consolidation, SRK Consulting, Chemnitz, Germany.

Holtz, R., and Kovacs, W. (1981). An Introduction to Geotechnical Engineering, *Prentice-Hall, Inc.,* Englewood Cliffs, New Jersey.

Huerta, A., Kriegsmann G., and Krizek R. (1988). Permeability and compressibility of slurries from seepage-induced consolidation, *Journal of Geotechnical Engineering*, 114(5), 614-627.

Imai, G. (1981). Experimental studies on sedimentation mechanism and sediment formation of clay materials, *Soils and Foundations*, 21(1), 7-20.

Ito, M., and Azam S. (2013). Large-strain consolidation modeling of mine waste tailings, *Environmental Systems Research*, 2:7.

James, M. (2004). Evaluating the liquefaction resistance of tailings from hard rock mining, *Proceedings Tailings and Mine Waste 2004*, A.A. Balkema Publishers, Vancouver, BC, Canada, pp. 89-99.

Jeeravipoolvarn, S., Scott, J.D., and Chalaturnyk, R.J. (2009). 10 m standpipe tests on soil sands tailings: long-term experimental results and prediction, *Canadian Geotechnical Journal*, 46: 875-888.

Koppula, S. D. (1970). The consolidation of soil in two dimensions and with moving boundaries, PhD Dissertation, Department of Civil Engineering, University of Alberta, Edmonton, Canada.

Miller, R. (2012). Evaluation of a three-dimensional model for slurry storage facilities, M.S. Thesis, Department of Civil, Environmental and Architectural Engineering, University of Boulder, Boulder, Colorado.

Mitchell, J. (1976). Fundamentals of Soil Behavior, *John Wiley & Sons, Inc*., New York.

McVay, M., Townsend, F., and Bloomquist, D. (1986), Quiescent consolidation of phosphatic waste clays, *Journal of Geotechnical Engineering*, 112(11), pp. 1033-1049.

Lara, J. and Barrera, S. (2000). Presas de Relaves con muros resistentes de arena, Experiencias de aplicación y posibilidad de uso en países andinos. Arcadis, Chile.

Liu, J. and Znidarcic, D. (1991). Modeling one-dimensional compression characteristics of soils, *Journal of Geotechnical Engineering*,117(1), 162-169

Pane, V. and Schiffman, R. (1981). A comparison between two theories of finite strain consolidation, *Soils and Foundations*, Japanese Society of Soil Mechanics and Foundation Engineering, 21(4).

Palomino, A. and Santamarina, C. (2005). Fabric map for kaolinite: effects of pH and ionic concentration on behavior, *Clays and Clays Minerals*, 53(3), 2009-222.

Priestley, D. (2011). Modeling multidimensional large strain consolidation of tailings, M.S. thesis, The Faculty of Graduate Studies, Mining Engineering, The University of British Columbia, Vancouver.

Priscu, C., (1999). Behavior of mine tailings dams under high tailings deposition rates, Ph.D. Thesis, Department of Mining and Metallurgical Engineering, McGill University, Montreal, Canada.

Schiffman, R., Vick, S., and Gibson, R. (1988). Behavior and properties of hydraulic fills. Hydraulic fill structures, *Conference of the American Society of Civil Engineer- American Institute of Mining, Metallurgical, and Petroleum Engineers (ASCE-AIME)*, Fort Collins, CO, pp. 166-202

Somogyi, F. (1980). Large-strain consolidation of fine-grained slurries, *Annual conference, Canadian Society for Civil Engineering*, Winnipeg, Canada.

Suthaker N., and Scott D. (1996). Measurement of hydraulic conductivity in oil sand tailings slurries, *Canadian Geotechnical Journal*, 33(4), 642-653.

Taylor, D. (1948). Fundamentals of Soil Mechanics, *Wiley*, New York.

Townsend, F.C., and McVay, M.C. (1990). SOA: Large strain consolidation predictions, *Journal of Geotechnical Engineering*, 116(2), pp. 222-243.

Vick, S. (1983). Planning, Design, and Analysis of Tailings Dams, *Wiley*, New York.

Wels, C., and Robertson, A. (2003). Conceptual model for estimating water recovery in tailings impoundments, *Proceedings Tailings and Mine Waste 2003*, A.A. Balkema Publishers, Vancouver, BC, Canada, pp. 87- 94.

Wels, C., Robertson, A., and Madariaga P. (2004). Water recovery study for Pampa Pabellon Tailings impoundment Collahuasi, Chile, *Proceedings Tailings and Mine Waste 2004, Taylor & Francis* , Vail, Colorado, US, pp. 77-86.

West, J. (2011). Decreasing metal ore grades, *Journal of Industry Ecology*, Yale University, 15(2), pp. 165-168.

Yao, D. and Znidarcic, D. (1997). User's manual for computer program CONDES0, Report prepared for Florida Institute of Phosphate Research, University of Colorado, Boulder, Colorado.

Znidarcic, D., Croce, P., Pane V., Ko H.Y., Olsen, H., and Schiffman, R. (1984). The theory of one-dimensional consolidation of saturated clays: III. Existing testing procedures and analyses, *Geotechnical Testing Journal, American Society for Testing and Materials*. Vol. 7(3), pp. 123-133.

Znidarcic, D., Abu-Hejleh N., Fairbanks T., and Robertson A. (1992). Consolidation characteristics determination for phosphatic clays, Vol 1 Seepage Induced Consolidation Test Equipment Description and Users Manual, Prepared for Florida Institute of Phosphate Research, University of Boulder, Boulder.

Znidarcic, D. (1999). Predicting the behavior of disposed dredging soils, *Geotechnical Engineering for Transportation Infrastructure*, Balkema, Rotterdam, pp. 877-886.

Znidarcic, D., Miller, R., Van Zyl, D., Fredlund, M., and Wells, S. (2011). Consolidation testing of oil sand fine tailings, *Proceedings Tailings and Mine Waste 2011*, Norman B. Keevil Institute of Mining Engineering, Vancouver, BC, Canada, pp. 251-257.

APPENDIX A: COLLECTION OF CONSOLIDATION CONSTITUTIVE PARAMETERS AND TMT GEOMETRY TAP

Table A.1. Compilation of consolidation constitutive parameters.

Label No.	Material [a]	Name	e_0 [b]	G_s	A	B	Z (kPa)	C (m/s)	D	Reference
1	Cu tailings	WT-2	1.71	2.77	1.3	-0.168	0.192	1.02×10^{-7}	3.42	Case study - Actual operation
2	Cu tailings	WT-1	1.29	2.73	1.03	-0.115	0.141	1.55×10^{-7}	2.80	Case study - Pilot plan
3	Cu tailings	OF	3.21	2.725	1.67	-0.127	0.006	4.62×10^{-8}	3.06	Case study - Pilot plan
4	Cu tailings	Sulfide tailings [c]	1.10	4.2	1.29	-0.071	9.402	5.25×10^{-8}	6.70	Priestley (2011)
5	Cu tailings	UBC tailings	1.35	2.65	1.18	-0.166	0.451	4.10×10^{-8}	2.74	Estepho (2014)
6	Au tailings	Gold tailings	1.03	2.64	4.01	-0.245	255.5	3.28×10^{-8}	4.84	Priestley (2011)
7	Au tailings	Gossan tailings [d]	2.00	3.00	1.97	-0.099	0.86	4.88×10^{-9}	4.82	Priestley (2011)
8	OS tailings	UBC-MFT 1	5.44	2.65	3.00	-0.177	0.035	1.40×10^{-11}	3.55	Estepho (2014)
9	OS tailings	UBC-MFT 2 (MFT)	5.26	2.65	3.52	-0.236	0.181	1.10×10^{-11}	3.79	Estepho (2014)
10	OS tailings	UBC-MFT 3	5.07	2.65	3.81	-0.285	0.365	2.80×10^{-11}	3.03	Estepho (2014)

[a] Cu= copper ; Au= gold; OS= oil sand

[b] Initial void ratio, $e_0=A.Z^B$

[c] From copper and zinc extraction

[d] From gold and silver extraction process

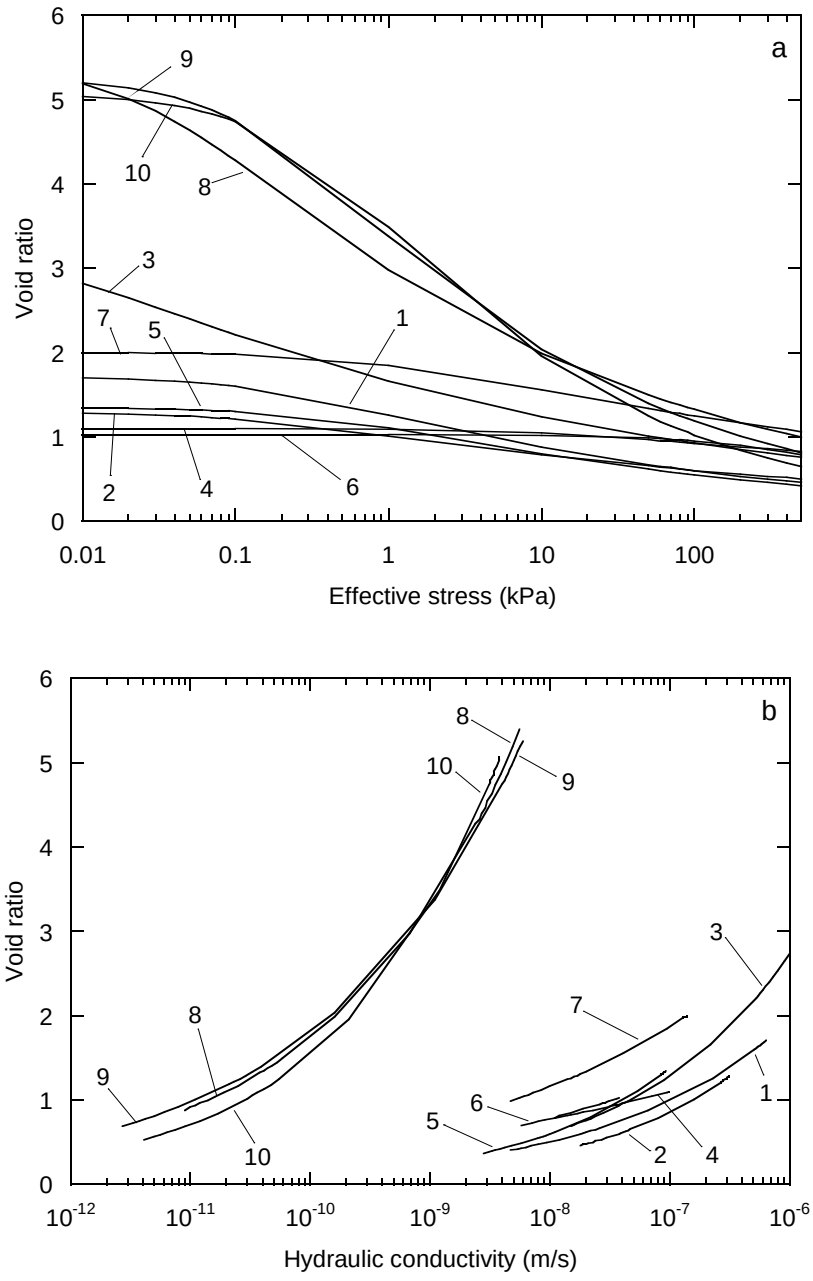

Fig. A.1. Compilation of constitutive relationships of mine tailings (Table A.1) (a) effective stress - void ratio relationship (b) hydraulic conductivity – void ratio relationship.

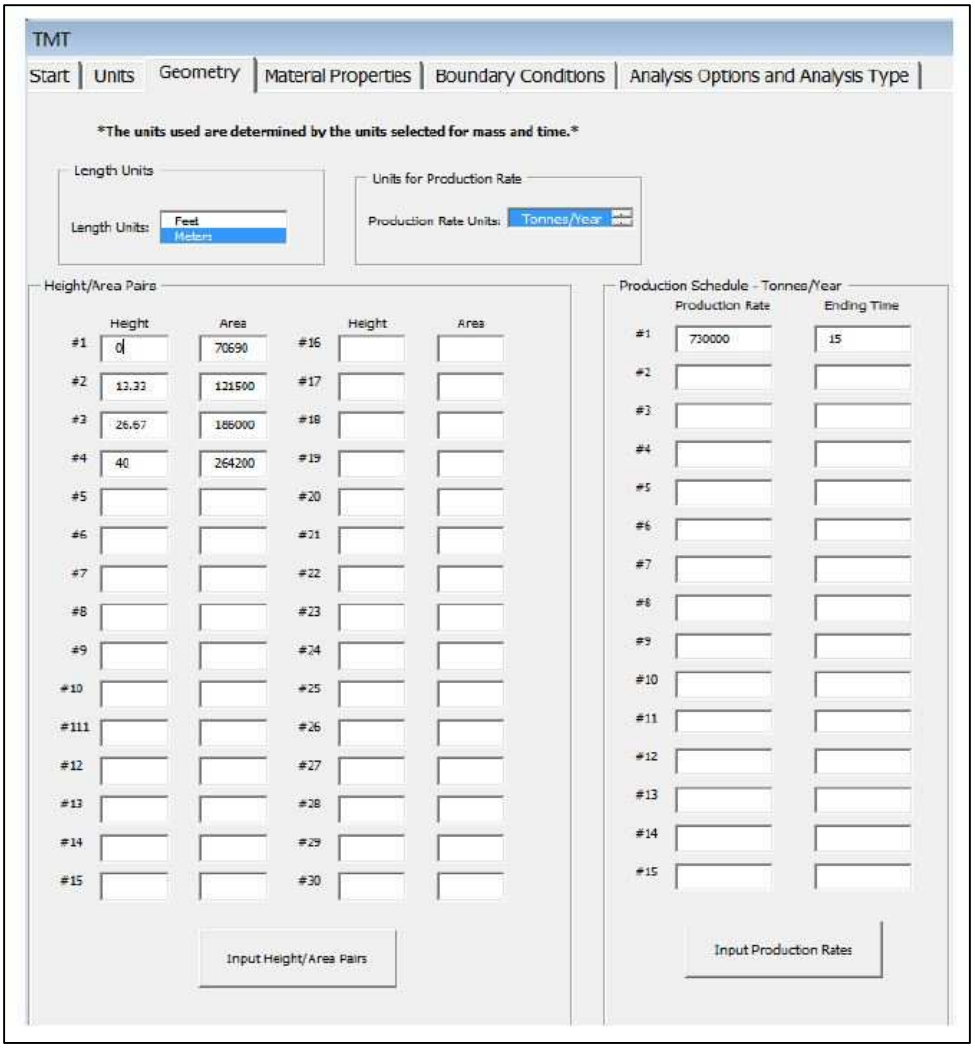

Fig. A.2. TMT geometry tab where height-area pairs and production schedule can be entered (figure from Miller 2012).